

# **Supplemental Material for Machine Learning Algorithms for Assisting Solvers for Constraint Satisfaction Problems**

**Morteza Kimiaeī** 

Fakultät für Mathematik, Universität Wien  
Oskar-Morgenstern-Platz 1, A-1090 Wien, Austria  
Email: [kimiaeim83@univie.ac.at](mailto:kimiaeim83@univie.ac.at)  
WWW: <http://www.mat.univie.ac.at/~kimiae>

**Vyacheslav Kungurtsev** 

Department of Computer Science, Czech Technical University  
Karlovo Namesti 13, 121 35 Prague 2, Czech Republic  
Email: [vyacheslav.kungurtsev@fel.cvut.cz](mailto:vyacheslav.kungurtsev@fel.cvut.cz)

## **Contents**

<b>1 ML, RL, and Deep NNs Background</b>	<b>3</b>
1.1 ML Foundations . . . . .	3
1.2 RL Principles and its Mathematical Foundations . . . . .	4
1.3 Technical Foundations of Deep NNs . . . . .	10
1.4 Brief Primer on DNNs . . . . .	10
<b>2 Mathematical Details of Learning Methods</b>	<b>12</b>
2.1 Training Dynamics of Deep NNs . . . . .	13
2.2 GNNs and Attention Models . . . . .	13
2.3 Differentiable Neural Logic and Notation . . . . .	17
<b>3 Classical Algorithms and developed software for CSPs</b>	<b>17</b>
3.1 Classical Algorithms for CSPs . . . . .	18
3.2 NNs as Enhancers for CSP Solvers . . . . .	27
3.3 Software using LCG and CDCL algorithms . . . . .	35

<b>4 Direct Solution Learning for CSPs</b>	<b>37</b>
4.1 Technical Formulation of the Solution Operator . . . . .	37
4.2 Supervised and Self-Supervised Learning for CSP . . . . .	37
4.3 End-to-End Neural Solvers . . . . .	39
4.4 Transfer and Meta-Learning across CSP Families . . . . .	39
<b>5 Learning Algorithms for Heuristic Search</b>	<b>40</b>
<b>6 Network Flow</b>	<b>43</b>
<b>7 GNNs for Graph Optimization</b>	<b>55</b>
7.1 Overview of Graph Optimization Problems . . . . .	55
7.2 Classical Graph Optimization Problems . . . . .	57
7.3 GNN Architectures for Graph Problems . . . . .	63
7.4 Applications . . . . .	64
7.4.1 GNNs for SPP . . . . .	65
7.4.2 GNNs for MST Learning . . . . .	65
7.4.3 GNNs for MFP/MCP Estimation . . . . .	66
7.4.4 GNNs for TSP Approximation . . . . .	66
<b>8 Extended Examples and Algorithms in DisP</b>	<b>67</b>
8.1 Background on Disjunctive Graphs and Logical Constraints . . . . .	67
8.2 Learning-Enhanced DisP: Extended Case Studies . . . . .	67
8.3 ML and RL Enhancements . . . . .	70
8.4 First-Order and Logical Constraint Satisfaction Problems (FOL-CSPs) . . . . .	71
<b>9 Empirical Evidence from the Literature</b>	<b>74</b>
9.1 RL for Search Heuristics . . . . .	74
9.2 ML for SAT and CSP Solvers . . . . .	74
9.3 Neural and Hybrid Optimization Frameworks . . . . .	75

This supplemental document provides the mathematical foundations, extended algorithmic descriptions, and detailed pseudocode underlying the learning-augmented CSP/SAT framework presented in the main paper. It includes complete specifications of Algorithms 1–18, covering the ML and RL components used for propagation, decision making, conflict analysis, restart control, structural instance analysis, and first-order CSP reasoning. The supplement further details the differentiable neural logic operators, reinforcement-learning update rules, graph-based representations, grounding procedures for FOL-CSPs, and disjunctive programming formulations. Additional flowcharts, examples, and empirical summaries are provided to support and clarify the methods discussed in the main article, whose e-print is available at [24]. The supplemental file itself is available at [25, suppMat.pdf].

## 1 ML, RL, and Deep NNs Background

ML and RL provide the statistical and decision-theoretic foundations for integrating adaptive intelligence into classical optimization frameworks such as Disjunctive Programming (**DisP**) and Boolean Satisfiability (**SAT**). Traditional solvers rely on fixed heuristics and symbolic inference, while ML and RL introduce mechanisms for learning from data and interaction, allowing systems to infer patterns, predict outcomes, and optimize decisions dynamically. The goal of this section is to present the conceptual and mathematical principles that enable learning components to operate within constraint solvers. The intuition is to treat ML and RL not as external add-ons but as complementary reasoning mechanisms that extend symbolic logic with statistical guidance in search, inference, and optimization. By reviewing the essential learning concepts and neural architectures here,

We prepare the reader to understand how these models and their mathematical formulations provided in Section 2—which now serves as the unified mathematical specification—are used in later solver components, where they guide propagation, decision making, and constraint satisfaction within hybrid symbolic–learning solvers.

### 1.1 ML Foundations

ML formalizes learning from data as an optimization problem over a hypothesis space of functions. Given a dataset  $\mathcal{D}_{\text{train}} = \{(x_i, y_i)\}$  drawn from an unknown distribution, the learner seeks a function  $f_\theta$  that minimizes the expected loss  $\mathbb{E}[\ell(f_\theta(x), y)]$ . Depending on the form of supervision, ML encompasses:

- **Supervised learning**, where labeled data  $(x_i, y_i)$  guide prediction (classification or regression);
- **Unsupervised learning**, which infers latent structure or representations without explicit targets (e.g., clustering, autoencoding);
- **Self-supervised or contrastive learning**, which generates supervisory signals directly from the data distribution.

Generalization—the ability to perform well on unseen instances—is achieved through regularization, inductive biases, and architectural constraints. These concepts underpin the predictive components used in learning-augmented solvers.

Detailed formulations of message-passing, attention, and regression models are provided in Section 2, which now serves as the unified mathematical specification for this background.

## 1.2 RL Principles and its Mathematical Foundations

RL extends ML to sequential decision-making under uncertainty. An agent interacts with an environment modeled as a Markov Decision Process (MDP)  $(\mathcal{S}, \mathcal{A}, \text{Pr}, R, \gamma)$ , observing states  $s_t$ , taking actions  $a_t$ , and receiving rewards  $r_t$ . The objective is to learn a policy  $\pi_\theta(a|s)$  that maximizes the expected discounted return  $J(\theta) = \mathbb{E}_{\pi_\theta}[\sum_t \gamma^t r_t]$ . Learning proceeds through experience, balancing exploration of new actions and exploitation of known good ones. Two complementary families of methods are widely used:

- **Value-based approaches**, which estimate optimal value functions  $Q^*(s, a)$  (e.g., Q-learning, DQN);
- **Policy-gradient and actor-critic approaches**, which directly optimize the policy parameters through gradient ascent.

RL formalizes optimization and control as a sequential decision-making process modeled by a Markov Decision Process (MDP)

$$\mathcal{M} = (\mathcal{S}, \mathcal{A}, \text{Pr}, R, \gamma),$$

where  $\mathcal{S}$  is the set of states,  $\mathcal{A}$  the set of actions,  $\text{Pr}(s'|s, a)$  the transition probability,  $R(s, a)$  the reward, and  $\gamma \in (0, 1]$  the discount factor. At time  $t$ , the agent observes state  $s_t$ , selects action  $a_t$ , receives reward  $r_t = R(s_t, a_t)$ , and transitions to  $s_{t+1}$ . The goal is to find a policy  $\pi_\theta(a|s)$  that maximizes the expected return

$$J(\theta) = \mathbb{E}_{\pi_\theta} \left[ \sum_{t=0}^T \gamma^t r_t \right].$$

For later reference, we define the *Monte Carlo return* as

$$R_t = \sum_{k=t}^T \gamma^{k-t} r_k,$$

which represents the discounted cumulative reward collected along a trajectory under policy  $\pi_\theta$ .

**Policy Gradient Theorem.** For a differentiable policy  $\pi_\theta$ , the gradient of the expected return is

$$\nabla_\theta J(\theta) = \mathbb{E}_{\pi_\theta} [\nabla_\theta \log \pi_\theta(a|s) Q^{\pi_\theta}(s, a)],$$

where  $Q^{\pi_\theta}(s, a)$  is the true action–value function under policy  $\pi_\theta$ , and  $V^{\pi_\theta}(s)$  is the corresponding state–value function estimating the expected return from state  $s$ . In practical actor–critic implementations, these functions are approximated by NNs  $Q_\psi(s, a)$  and  $V_\phi(s)$  with parameters  $\psi$  and  $\phi$ . The advantage estimate is then computed as

$$\hat{A}_t = Q_\psi(s_t, a_t) - V_\phi(s_t),$$

which measures how much better an action performed is compared with the critic’s baseline expectation.

**Value-Based Methods.** In Q-learning, the agent estimates the optimal action–value function  $Q^*(s, a)$ , which satisfies the Bellman optimality equation. The tabular update rule is

$$Q(s, a) \leftarrow (1 - \alpha)Q(s, a) + \alpha [r + \gamma \max_{a'} Q(s', a')],$$

where  $\alpha$  is the learning rate and  $\gamma \in (0, 1]$  is the discount factor weighting future rewards. In function-approximation settings such as Deep Q-Networks (DQN), the value function is represented by an NN  $Q_\psi(s, a)$  parameterized by  $\psi$ . Its parameters are optimized by minimizing the temporal-difference loss

$$L(\psi) = \mathbb{E} [(r + \gamma \max_{a'} Q_{\psi^-}(s', a') - Q_\psi(s, a))^2],$$

where  $\psi^-$  denotes the frozen target-network parameters, and  $Q_\psi(s, a)$  serves as an approximation of the true  $Q^*(s, a)$  [52].

Algorithm 1 summarizes the A2C procedure. In step (S0<sub>1</sub>), the actor–critic networks and learning rates are initialized. During (S1<sub>1</sub>), the current policy  $\pi_\theta$  interacts with the environment to collect trajectories of states, actions, and rewards. (S2<sub>1</sub>) computes the discounted returns and advantage estimates  $\hat{A}_t$

using the critic's value predictions. The actor parameters are then updated in (S3<sub>1</sub>) through a policy-gradient ascent step that reinforces actions with positive advantages, while the critic parameters are refined in (S4<sub>1</sub>) by minimizing the mean-squared error between predicted and observed returns. Finally, (S5<sub>1</sub>) synchronizes gradients across multiple trajectories to ensure stable, parallel updates.

---

**Algorithm 1 Advantage Actor–Critic (A2C) [35]**


---

(S0<sub>1</sub>) Initialize actor parameters  $\theta$ , critic parameters  $\phi$ , learning rates  $(\alpha_\theta, \alpha_\phi)$ , and discount factor  $\gamma$ .

**repeat**

(S1<sub>1</sub>) Run current policy  $\pi_\theta(a|s)$  in the environment for  $T$  steps. Collect trajectories  $\{(s_t, a_t, r_t, s_{t+1})\}_{t=1}^T$  and compute the Monte Carlo return

$$R_t = \sum_{k=t}^T \gamma^{k-t} r_k, \quad r_k = R(s_k, a_k),$$

where  $R(s, a)$  is the immediate reward function defined in the MDP, and  $R_t$  denotes its discounted cumulative estimate over a sampled trajectory, which is the empirical return computed via Monte Carlo rollout, distinguishing it from the reward function  $R(s, a)$  that defines instantaneous feedback.

(S2<sub>1</sub>) Estimate advantages using the critic network:

$$\hat{A}_t = R_t - V_\phi(s_t).$$

(S3<sub>1</sub>) Update actor parameters by ascending the policy-gradient objective:

$$\theta \leftarrow \theta + \alpha_\theta \nabla_\theta \log \pi_\theta(a_t | s_t) \hat{A}_t.$$

(S4<sub>1</sub>) Update critic parameters by minimizing the value loss:

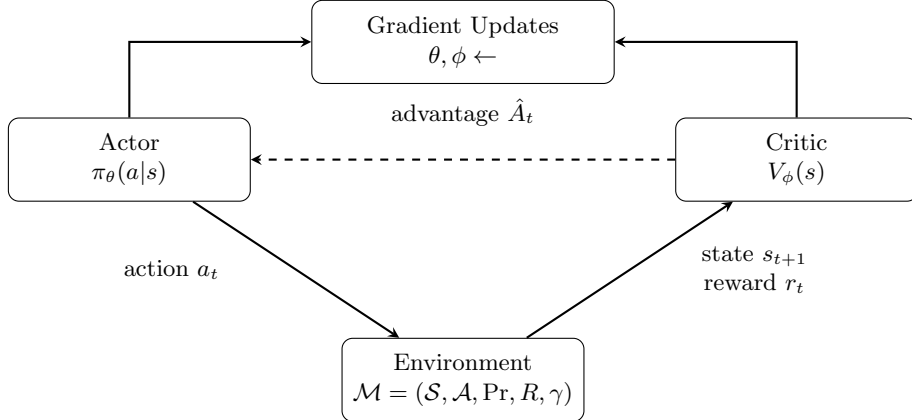
$$\phi \leftarrow \phi - \alpha_\phi \nabla_\phi (V_\phi(s_t) - R_t)^2.$$

(S5<sub>1</sub>) Optionally synchronize gradients or parameter averages across multiple parallel trajectories (synchronous update).

**until** policy convergence or training budget exhausted.

---

Figure 1 illustrates how the actor and critic cooperate in A2C: the actor generates actions, the critic provides advantage feedback, and both are updated through gradient steps.



Collect trajectories  $\{(s_t, a_t, r_t)\}$  and update actor via policy gradient, critic via value loss.

Figure 1: **Advantage Actor–Critic (A2C)** [35]. The actor interacts with the environment to collect trajectories, while the critic evaluates state values to compute the advantage  $\hat{A}_t$ . Both networks update synchronously to improve the policy.

Algorithm 2 outlines the PPO update process. In step (S0<sub>2</sub>), the policy and value networks are initialized together with learning rates, clipping constant  $\epsilon$ , and discount factor  $\gamma$ . During (S1<sub>2</sub>), the current policy  $\pi_\theta$  interacts with the environment to generate trajectories and compute the corresponding discounted returns  $R_t$ . Step (S2<sub>2</sub>) estimates advantages  $\hat{A}_t$  using the critic’s predictions  $V_\phi(s_t)$ . The policy parameters are then updated in (S3<sub>2</sub>) by maximizing the clipped objective (1), where the ratio  $\rho_t(\theta)$  measures the change between new and old policies and the clipping term limits large updates to stabilize learning. Finally, the critic is refined in (S4<sub>2</sub>) by minimizing the value loss  $L_V(\phi) = \mathbb{E}_t[(V_\phi(s_t) - R_t)^2]$ . The procedure repeats until the policy converges or the training budget is exhausted.

**Risk-Sensitive Extensions.** In distributional RL, the return from state-action pair  $(s, a)$  is treated as a random variable rather than a scalar expectation. Let  $Z^\pi(s, a)$  denote the return distribution under policy  $\pi$ , defined as the distribution of discounted cumulative rewards obtained by following  $\pi$  after taking action  $a$  in state  $s$ . The stochastic Bellman operator governing its evolution is

$$\mathcal{T}^\pi Z(s, a) = R(s, a) + \gamma Z^\pi(s', a'),$$

where  $R(s, a)$  is the random immediate reward,  $Z(s, a)$  represents a generic (estimated) return variable, and  $\gamma \in (0, 1]$  is the discount factor. A risk-sensitive

---

**Algorithm 2** Proximal Policy Optimization (PPO) [43]

---

(S0<sub>2</sub>) Initialize policy parameters  $\theta$ , value function parameters  $\phi$ , clipping constant  $\epsilon > 0$ , learning rates  $(\alpha_\theta, \alpha_\phi)$ , and discount factor  $\gamma$ .

**repeat**

(S1<sub>2</sub>) Run policy  $\pi_\theta$  in the environment for  $T$  steps, collect transitions  $(s_t, a_t, r_t, s_{t+1})$  and compute discounted returns  $R_t = \sum_{k=t}^T \gamma^{k-t} r_k$ .

(S2<sub>2</sub>) Estimate advantages  $\hat{A}_t = R_t - V_\phi(s_t)$ .

(S3<sub>2</sub>) Compute the probability ratio  $\rho_t(\theta) = \pi_\theta(a_t|s_t)/\pi_{\theta_{\text{old}}}(a_t|s_t)$ , where  $\pi_{\theta_{\text{old}}}$  denotes the policy before the current update. Update  $\theta$  by maximizing the clipped objective:

$$L^{\text{CLIP}}(\theta) = \mathbb{E}_t \left[ \min \left( \rho_t(\theta) \hat{A}_t, \text{clip}(\rho_t(\theta), 1 - \epsilon, 1 + \epsilon) \hat{A}_t \right) \right]. \quad (1)$$

The clipping term stabilizes learning by preventing excessively large policy updates that could degrade performance.

(S4<sub>2</sub>) Update  $\phi$  by minimizing  $L_V(\phi) = \mathbb{E}_t [(V_\phi(s_t) - R_t)^2]$ .

**until** policy convergence or training budget exhausted.

---

objective can be formulated using the Conditional Value-at-Risk (CVaR),

$$\text{CVaR}_\alpha(Z) = \mathbb{E}[Z \mid Z \leq F_Z^{-1}(\alpha)], \quad (2)$$

where  $\alpha \in (0, 1)$  specifies the risk level. The CVaR quantifies the expected loss (or return) in the worst  $\alpha$ -fraction of cases, providing a principled measure of tail risk widely used in robust and safety-critical learning [53]. In risk-averse optimization, the objective is typically to minimize  $\text{CVaR}_\alpha(Z)$ , thereby reducing the expected loss in the worst  $\alpha$ -fraction of outcomes, rather than maximizing the mean return.

Figure 2 visualizes the PPO framework, where policy updates are constrained by a clipping term to ensure stable, monotonic improvement of the actor network.

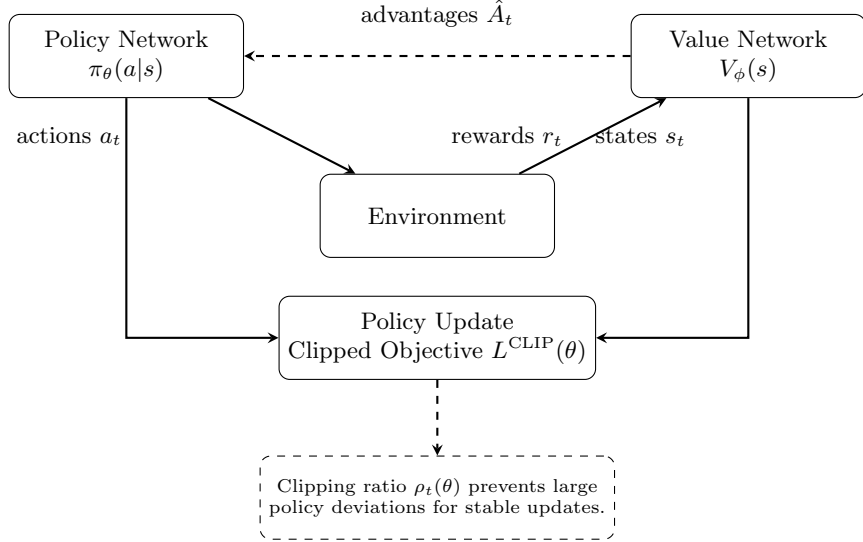


Figure 2: Structure of the PPO algorithm. The actor and critic networks generate trajectories, compute advantages, and perform gradient updates on the clipped objective  $L^{\text{CLIP}}(\theta)$  to stabilize learning.

**Algorithm Configuration.** Many solvers expose continuous or discrete parameters  $\boldsymbol{\theta} \in \Theta$  that influence performance. The algorithm-configuration problem seeks

$$\boldsymbol{\theta}^* = \underset{\boldsymbol{\theta} \in \Theta}{\operatorname{argmin}} \mathbb{E}_{\phi \sim \mathcal{D}_{\text{inst}}} [T(\phi, \boldsymbol{\theta})],$$

where  $T(\phi, \boldsymbol{\theta})$  is the runtime on instance  $\phi$ , and  $\mathcal{D}_{\text{inst}}$  denotes the distribution of instances. This optimization viewpoint links ML model selection with solver parameter tuning, discussed later. Note that  $\mathcal{D}_{\text{inst}}$  here denotes an instance distribution, distinct from the training dataset  $\mathcal{D}_{\text{train}}$  used in supervised learning earlier.

**Reward Shaping and Training Loop.** In optimization-oriented RL, the reward  $r_t$  often reflects the improvement of an objective function over time. If  $J_t$  denotes the current objective value, a natural shaping scheme is

$$r_t = J_{t-1} - J_t,$$

so that positive rewards correspond to reductions in the objective (i.e., performance improvement). Each training iteration alternates between data collection under the current policy, advantage estimation, and parameter updates using Algorithm 2. This iterative loop constitutes the backbone of RL integration in subsequent sections.

### 1.3 Technical Foundations of Deep NNs

Deep Neural Networks (DNNs) provide the parametric foundation for modern ML models. They generalize classical function-approximation schemes by composing multiple layers of nonlinear transformations that progressively extract hierarchical features from data. A standard feedforward network defines a differentiable mapping

$$f_\theta : \mathbb{R}^{d_{\text{in}}} \rightarrow \mathbb{R}^{d_{\text{out}}}, \quad f_\theta(x) = \phi_L \circ \phi_{L-1} \circ \cdots \circ \phi_1(x),$$

where each layer  $\phi_\ell$  is parameterized by a weight matrix  $W_\ell$  and bias vector  $b_\ell$ , and applies an elementwise nonlinearity  $\sigma$ :

$$\phi_\ell(x) = \sigma(W_\ell x + b_\ell), \quad \sigma(z) \in \{\text{ReLU}(z), \tanh(z), \text{sigmoid}(z)\}.$$

The parameter set  $\theta = \{W_\ell, b_\ell\}_{\ell=1}^L$  is learned from data by minimizing an empirical loss

$$L(\theta) = \frac{1}{|\mathcal{D}_{\text{train}}|} \sum_{(x_i, y_i) \in \mathcal{D}_{\text{train}}} \ell(f_\theta(x_i), y_i),$$

where  $\ell(\cdot, \cdot)$  measures prediction discrepancy (e.g., cross-entropy or mean-squared error). Parameter updates follow gradient-based optimization such as stochastic gradient descent (SGD) or adaptive methods like Adam [26]:

$$\theta \leftarrow \theta - \eta \nabla_\theta L(\theta),$$

where  $\eta > 0$  denotes the learning rate.

### 1.4 Brief Primer on DNNs

**Representation Learning.** Each hidden layer learns intermediate features that transform raw inputs into more abstract, task-relevant representations. Lower layers typically encode local or syntactic patterns (e.g., edge or clause statistics), while deeper layers capture global semantic or relational structure. The universal-approximation theorem guarantees that sufficiently wide DNNs can approximate any continuous mapping on a compact domain, providing a theoretical justification for their expressive power.

**Regularization and Generalization.** To prevent overfitting, several mechanisms are commonly used: weight-decay regularization ( $\lambda \|\theta\|_2^2$ ), dropout (stochastic node omission), and batch normalization (adaptive rescaling of activations). These techniques improve generalization across problem instances  $\phi \sim \mathcal{D}_{\text{inst}}$ .

**Architectural Variants.** Beyond fully connected (dense) networks, specialized architectures exploit problem structure:

- **Convolutional Neural Networks (CNNs)** share weights across local neighborhoods, supporting translation invariance.
- **Recurrent Neural Networks (RNNs)** and gated variants (LSTM, GRU) capture temporal or sequential dependencies through recurrent state updates.
- **GNNs** extend these principles to relational structures (see Section 2), which provides the corresponding mathematical formulations.

**Backpropagation in Learning-Augmented Solvers.** In neural-augmented solvers, the policy parameters  $\theta$  are optimized via stochastic gradient descent:

$$\theta \leftarrow \theta - \eta \nabla_{\theta} \mathcal{L}(\pi_{\theta}(\mathcal{A}_p), y),$$

where  $\mathcal{L}$  measures the discrepancy between the learned policy  $\pi_{\theta}$  and a target decision  $y$ . This continuous update mechanism complements the discrete backtracking of classical solvers, linking symbolic search with differentiable learning.

For the full mathematical derivations of gradient propagation, graph-neural architectures, and reinforcement-learning algorithms, (see Section 2), which provides the corresponding mathematical formulations.

**Integration and Notation.** ML components act as predictive heuristics that refine fixed solver rules (e.g., variable scoring or branching order), while RL agents learn adaptive control policies through sequential interaction. Table 1 summarizes the notation used throughout this work.

Table 1: Summary of notation for ML and RL components used in this work.

Symbol	Meaning
$f_{\theta}$	parameterized machine learning model.
$\pi_{\phi}(a s)$	Policy (actor) parameterized by $\phi$ (sometimes denoted $\pi_{\theta}$ in PPO/A2C formulations).
$V_{\phi}(s)$	State-value function (critic).
$Q_{\psi}(s, a)$	Action-value function.
$\hat{A}_t = R_t - V_{\phi}(s_t)$	Advantage estimate measuring deviation from baseline performance.
$\rho_t$	PPO probability ratio $\pi_{\theta}(a_t s_t)/\pi_{\theta_{\text{old}}}(a_t s_t)$ .
$\epsilon$	PPO clipping constant controlling update bounds.

Continued on next page

Table 1 – continued from previous page

Symbol	Meaning
$\alpha_\theta, \alpha_\phi$	Learning rates for actor and critic networks.
$\mathcal{M} = (\mathcal{S}, \mathcal{A}, \text{Pr}, R, \gamma)$	Markov Decision Process (MDP) tuple: states, actions, transitions, rewards, and discount factor.
$s_t, a_t, r_t$	State, action, and reward at time step $t$ .
$T$	Rollout length or time horizon.
$h_v$	Learned node embedding of vertex $v$ in a GNN.
$\mathcal{N}(v)$	Neighborhood of node $v$ .
$\mathbf{W}$	Learnable weight matrix used in message passing.
$r_t$	Stochastic reward signal in bandit and RL settings.
$\boldsymbol{\theta}$	Tunable solver or model configuration parameters.
$\phi_{\text{msg}}, \phi_{\text{upd}}$	Message and update functions in GNNs.
$\phi_{\text{read}}$	Readout operator aggregating node embeddings.
$c$	Temperature coefficient controlling sigmoid smoothness in dNL.
<code>node2vec</code>	Random-walk-based node-embedding method producing input features $x_i$ for graph models.
<code>pointer attention</code>	Attention mechanism used in sequence decoders to focus on selected elements during output generation [55].
$\mathcal{C}_{\text{working}}$	Working clause set maintained during search in SAT solvers.
<code>trial</code>	Record of assigned literals and their corresponding decision levels.
LBD	Literal Block Distance, a metric for clause activity in conflict analysis.
$\eta$	Solver or hyperparameter configuration vector (distinct from $\theta$ ).

## 2 Mathematical Details of Learning Methods

This section provides additional mathematical formulations and algorithmic details that complement Section 1. It expands on gradient-based learning dynamics, graph neural architectures, attention mechanisms, and reinforcement-learning procedures that form the computational foundation for hybrid symbolic–learning solvers.

## 2.1 Training Dynamics of Deep NNs

Learning proceeds via *backpropagation*, which applies the chain rule to propagate gradients from output to input layers:

$$\frac{\partial L}{\partial W_\ell} = \frac{\partial L}{\partial h_{\ell+1}} \frac{\partial h_{\ell+1}}{\partial h_\ell} \frac{\partial h_\ell}{\partial W_\ell}, \quad h_{\ell+1} = \sigma(W_\ell h_\ell + b_\ell).$$

This recursive update mechanism enables end-to-end differentiability across all parameters. In hybrid optimization frameworks, such differentiability permits integrating DNN components with symbolic solvers via gradient-based feedback.

## 2.2 GNNs and Attention Models

A supervised ML model learns a parametric mapping  $f_\theta : \mathcal{X} \rightarrow \mathcal{Y}$ , where  $\mathcal{X}$  denotes the input space and  $\mathcal{Y}$  the prediction target. The model parameters  $\theta$  are optimized using the standard supervised learning objective  $L(\theta)$  defined in Section 1, typically minimized by stochastic gradient descent (SGD) or adaptive methods such as Adam [26].

**Classification Models.** When the prediction target is categorical, ML models often use the softmax mapping to represent class probabilities

$$\Pr(y = k \mid \mathbf{x}) = \frac{\exp(\mathbf{w}_k^\top \mathbf{x} + b_k)}{\sum_{j=1}^K \exp(\mathbf{w}_j^\top \mathbf{x} + b_j)}, \quad (3)$$

where  $\mathbf{w}_k \in \mathbb{R}^d$  and  $b_k \in \mathbb{R}$  are learned parameters for class  $k$ . This model underlies instance classification and solver-selection tasks introduced later.

**GNN Representations.** For graph-structured inputs  $G = (V, E)$ , ML models often employ GNNs to capture relational dependencies between variables or constraints. Given node embeddings  $h_v^{(k)} \in \mathbb{R}^d$  at layer  $k$ , each iteration of message passing is defined by

$$m_v^{(k)} = \sum_{u \in \mathcal{N}(v)} \phi_{\text{msg}}(h_u^{(k)}, e_{uv}), \quad h_v^{(k+1)} = \phi_{\text{upd}}(h_v^{(k)}, m_v^{(k)}), \quad (4)$$

for all  $v \in V$ , where  $\phi_{\text{msg}}$ ,  $\phi_{\text{upd}}$ , and  $\phi_{\text{read}}$  are learnable neural functions (typically small MLPs), and  $e_{uv}$  encodes edge features such as precedence or resource type (the readout operator  $\phi_{\text{read}}$  aggregates node embeddings into a

fixed-size vector representation – e.g., mean, sum, or attention pooling – ensuring permutation invariance). A global graph representation is obtained through a permutation-invariant readout,

$$h_G = \phi_{\text{read}} \left( \{h_v^{(K)} \mid v \in V\} \right),$$

used as input to downstream decision models. Permutation invariance ensures that the learned graph representation remains consistent under node reordering. Here  $K$  denotes the total number of message-passing layers (or iterations) in the GNN, so that  $h_v^{(K)}$  is the final embedding of node  $v$  after  $K$  propagation steps.

**node2vec Embeddings.** The `node2vec` algorithm [21] learns continuous vector representations of nodes in a graph by simulating biased random walks that capture both local and global structure. Formally, let  $\mathcal{G} = (V, E)$  be a graph, and let  $\mathcal{N}_r(v) = (v_1, v_2, \dots, v_r)$  denote a length- $r$  random walk starting from node  $v \in V$ . The objective is to learn an embedding function

$$f : V \rightarrow \mathbb{R}^d$$

that maximizes the likelihood of preserving network neighborhoods under a skip-gram model:

$$\max_f \sum_{v \in V} \sum_{u \in \mathcal{N}_r(v)} \log \Pr(u \mid f(v)), \quad \Pr(u \mid f(v)) = \frac{\exp(f(u)^\top f(v))}{\sum_{w \in V} \exp(f(w)^\top f(v))}. \quad (5)$$

Here,  $\mathcal{N}_r(v)$  denotes the multiset of nodes visited within a random walk of length  $r$  starting from node  $v$ , and  $(p, q)$  are the return and in-out parameters that control the breadth-first and depth-first exploration biases controlling whether the random walk revisits nearby nodes or explores distant ones. The resulting embeddings  $f(v)$  serve as dense feature vectors for each node, used in subsequent graph-based learning tasks.

**Attention Mechanisms.** Transformer-based architectures generalize GNN aggregation through scaled dot-product attention:

$$\text{attn}(Q, K, V) = \text{softmax} \left( \frac{QK^\top}{\sqrt{d_k}} \right) V, \quad (6)$$

where  $Q, K, V \in \mathbb{R}^{n \times d_k}$  are the query, key, and value matrices obtained by linear projections of node features, and  $d_k$  is the key embedding dimension. This operator allows learning global dependencies over disjunctive or clause graphs while preserving differentiability.

Let  $\text{Enc}_\theta : \mathbb{R}^{n \times d_x} \rightarrow \mathbb{R}^{n \times d_z}$  denote the Transformer encoder parameterized by  $\theta$ , which computes a contextual embedding of the input  $X$ :

$$\text{Enc}_\theta(X) = \text{FFN}(\text{attn}(Q, K, V)), \quad (7)$$

where  $\text{attn}(Q, K, V)$  is the multi-head attention output defined in (6). The feed-forward network (FFN) applies non-linear transformations and residual connections, producing contextualized embeddings  $\text{Enc}_\theta(X)$  that capture dependencies among all input elements.

**Pointer Attention.** The pointer attention mechanism extends (6) by using attention weights to select a single element from the encoder outputs rather than computing a weighted sum. At decoding step  $t$ , the model assigns a probability distribution over encoder positions:

$$\alpha_{ti} = \frac{\exp((W_Q q_t)^\top (W_K x_i))}{\sum_j \exp((W_Q q_t)^\top (W_K x_j))}, \quad \Pr(a_t = i) = \alpha_{ti},$$

where  $q_t \in \mathbb{R}^{d_k}$  is the decoder query vector at step  $t$ ,  $x_i \in \mathbb{R}^{d_x}$  is the encoder representation of element  $i$ , and  $W_Q \in \mathbb{R}^{d_k \times d_q}$  and  $W_K \in \mathbb{R}^{d_k \times d_x}$  are learned projection matrices for the query and key transformations. The coefficient  $\alpha_{ti}$  denotes the probability of selecting encoder position  $i$ , and  $a_t$  represents the index of the element chosen at decoding step  $t$ . This mechanism, introduced by [55], enables a decoder to “point” directly to variables, operations, or clauses during sequential decision making, a capability later exploited in the attention-based scheduling and branching algorithms.

**Logistic Regression.** For binary prediction problems, such as polarity estimation in SAT solvers, a logistic model computes

$$\Pr(x_i = 1 | \mathbf{z}_i) = \frac{1}{1 + e^{-(\mathbf{v}^\top \mathbf{z}_i + c)}}, \quad (8)$$

where  $\mathbf{z}_i$  are the feature vectors of variable  $x_i$ ,  $\mathbf{v}$  are learned weights, and  $c$  is a bias term. This formulation reappears in the polarity-prediction heuristics described later in this section.

**Clause Utility Regression.** Clause retention and deletion decisions can be guided by a learned estimate of each clause’s expected utility. Let  $C$  denote a learned clause characterized by features such as its size  $|C|$ , Literal Block Distance  $\text{LBD}(C)$ , age, and activity score. A regression or neural model predicts a scalar utility value

$$u(C) = f_\theta([\text{LBD}(C), |C|, \text{age}(C), \text{activity}(C)]),$$

where  $f_\theta$  is a parametric function (e.g., a multilayer perceptron) with learnable parameters  $\theta$ . Clauses with higher predicted utility are prioritized during propagation and conflict analysis, while those with low utility are deprioritized or removed. This formulation provides a unified learning interface for clause management, referenced later in Algorithm 13.

**Online Learning and Bandit Models.** Some decision processes, such as variable selection or parameter tuning, can be formalized as multi-armed bandit problems. At each round  $t$ , the learner chooses an action (or arm)  $a_t$  and observes a stochastic reward  $r_t$ . A common strategy is the Upper Confidence Bound (UCB) policy

$$a_t = \operatorname{argmax}_i \left( Q_i + \beta \sqrt{\frac{\ln t}{n_i}} \right),$$

where  $Q_i$  is the estimated reward of arm  $i$ ,  $n_i$  counts how many times arm  $i$  has been selected, and  $\beta > 0$  controls exploration versus exploitation. Action values are updated incrementally by

$$Q_i \leftarrow Q_i + \eta(r_t - Q_i),$$

where  $\eta$  is the learning rate. The objective is to maximize the expected cumulative reward over a time horizon  $T$

$$\max_{\pi} \mathbb{E}_{\pi} \left[ \sum_{t=0}^T r_t \right],$$

where  $\pi$  denotes the stochastic decision policy balancing exploration and exploitation. This framework underlies adaptive heuristics such as learning-rate branching and algorithm configuration used in later sections.

**Learning Rate Branching (LRB).** A practical instance of bandit-based decision making used in modern SAT solvers is the LRB heuristic. Each variable  $x_i$  corresponds to an arm with reward  $r_t^{(i)}$  inversely proportional to the conflict depth after branching. At iteration  $t$ , the policy selects arm  $i$  according to

$$\Pr(a_t = i) = \frac{\exp(Q_t(i)/\tau)}{\sum_j \exp(Q_t(j)/\tau)},$$

where  $Q_t(i)$  is the estimated utility and  $\tau > 0$  controls exploration. Action values are updated incrementally,

$$Q_{t+1}(i) \leftarrow (1 - \alpha)Q_t(i) + \alpha r_t^{(i)}.$$

This bandit-based mechanism balances exploration and exploitation in variable selection, serving as a prototype for adaptive branching in CSP/SAT solvers (detailed later in Algorithm 12).

## 2.3 Differentiable Neural Logic and Notation

Differentiable Neural Logic(dNL) provides a continuous counterpart to symbolic reasoning, enabling smooth logical operations within gradient-based training. Logical relations are represented through differentiable operators:

$$f_{\text{conj}}(x) = \prod_i (1 - m_i(1 - x_i)), \quad f_{\text{disj}}(x) = 1 - \prod_i (1 - m_i x_i), \quad (9)$$

where  $x_i \in [0, 1]$  denotes a soft truth value, and  $m_i = \sigma(cw_i) \in [0, 1]$  is a learned weighting coefficient obtained via a sigmoid activation with temperature parameter  $c > 0$ . These functions provide smooth relaxations of Boolean conjunction ( $\wedge$ ) and disjunction ( $\vee$ ), thereby enabling continuous optimization over logical expressions. The temperature coefficient  $c$  controls the smoothness of the logical transition: larger values of  $c$  make the soft logic closer to crisp Boolean behavior. These differentiable operators form the foundation of neural–symbolic reasoning frameworks for continuous logical optimization.

Given a clause  $C$  with soft literal activations  $\{x_i\}_{i \in C}$ , the differentiable logical loss is defined as

$$L_{\text{logic}} = \sum_{C \in \mathcal{C}} (1 - f_{\text{disj}}(\{x_i : i \in C\})), \quad (10)$$

which penalizes violated or weakly satisfied disjunctions. The loss is 0 precisely when all clauses are fully satisfied under the current soft assignments. This quantity is used in Algorithms 17 during the gradient-based update step (S2<sub>17</sub>).

This section establishes the ML and RL terminology, notation, and algorithms referenced in later integrations with DisP and SAT frameworks.

## 3 Classical Algorithms and developed software for CSPs

Classical CSP solving can be interpreted as a graph–search problem over the space of partial assignments. Each node in the search tree corresponds to a partial assignment  $\mathcal{A}_p \subseteq \mathcal{A}$ , and each edge represents the assignment of a new variable value consistent with the constraints so far. Let  $\mathcal{A}_p(x_i) = v$  denote that variable  $x_i$  has been assigned value  $v$ .

Formally, we define the *search tree* as

$$T = (V_T, E_T), \quad V_T = \{\mathcal{A}_p \mid \mathcal{A}_p : \mathcal{X}' \subseteq \mathcal{X}, \mathcal{A}_p(x_i) \in \mathcal{D}(x_i)\},$$

where  $(\mathcal{A}_p, \mathcal{A}'_p) \in E_T$  if  $\mathcal{A}'_p = \mathcal{A}_p \cup \{(x_i, v)\}$  for some unassigned  $x_i$  and  $v \in \mathcal{D}(x_i)$  consistent with all  $c_j \in \mathcal{C}$ . A leaf node represents either a conflict (dead end) or a full assignment  $\mathcal{A}$ .

### 3.1 Classical Algorithms for CSPs

Table 2: Asymptotic time and space complexities of the six classical algorithms discussed in this section, based on [4, 41]. Here,  $b$  is the branching factor,  $d$  the depth of the shallowest solution,  $m$  the maximum search depth,  $n$  the number of variables,  $c$  the number of constraints, and  $|\mathcal{D}|$  the maximum domain size.

Algorithm	Time Complexity	Space Complexity
AC-3	$O(c \mathcal{D} ^3)$	$O(c \mathcal{D} ^2)$
BTS	$O( \mathcal{D} ^n)$ (worst case)	$O(n)$
BB	exponential in $n$	$O(n)$
BFS	$O(b^{d+1})$	$O(b^{d+1})$
DFS	$O(b^m)$	$O(bm)$
A*	$O(b^d)$ (worst case)	$O(b^d)$

Table 2 summarizes the asymptotic time and space complexities of the six foundational algorithms discussed in this chapter. As described by [41, Ch. 5.2], the constraint-propagation algorithm AC-3 runs in  $O(c|\mathcal{D}|^3)$  time and  $O(c|\mathcal{D}|^2)$  space, providing efficient domain pruning for binary constraints. Search-based procedures such as BTS, BFS, and DFS exhibit exponential worst-case complexity [41, Chs. 3.4–3.6, 5.3], reflecting the NP-completeness of general CSPs. BB inherits the exponential worst-case growth of DFS, but often achieves substantial practical gains through bounding and pruning strategies [4, 41, Ch. 4]. The informed search algorithm A\* maintains the same exponential bound in the worst case, but can achieve dramatic speedups when using consistent heuristics.

These asymptotic limits underscore why subsequent sections introduce heuristic, learning-based, and neural approaches. By guiding search with data-driven inference, such methods aim to mitigate exponential growth and improve the scalability of solver decisions.

**Arc Consistency and the AC-3 Algorithm.** Among propagation methods, the AC-3 procedure (=Algorithm 3) is one of the most widely used for establishing consistency in binary CSPs. It operates by iteratively enforcing consistency on every directed arc  $(X_i, X_j)$  in the constraint graph. Whenever a value in the domain of  $X_i$  is found inconsistent with all values of  $X_j$ , it is pruned, and the neighboring arcs of  $X_i$  are reinserted for reconsideration. This process continues

until no domain reductions occur. AC-3 guarantees that all binary constraints are locally consistent and terminates with a consistent domain assignment or detects inconsistency if any domain becomes empty.

---

**Algorithm 3 Arc Consistency Algorithm (AC-3)**


---

```

(S03) Initialize a queue  $Q$  with all arcs  $(X_i, X_j)$  in the constraint graph.

repeat
    (S13) Remove an arc  $(X_i, X_j)$  from  $Q$ .
    (S23) For each value  $x \in \mathcal{D}(X_i)$ , check whether there exists a value  $y \in \mathcal{D}(X_j)$  such that the constraint between  $X_i$  and  $X_j$  is satisfied. If no such  $y$  exists, remove  $x$  from  $\mathcal{D}(X_i)$ .
    (S33) If  $\mathcal{D}(X_i)$  was reduced, then for each neighbor  $X_k$  of  $X_i$  (except  $X_j$ ), add  $(X_k, X_i)$  to  $Q$ .
until  $Q$  is empty.
(S43) If any domain  $\mathcal{D}(X_i)$  becomes empty, return inconsistent.
Otherwise, all domains are arc-consistent; return consistent.

```

---

**Backtracking Search (BTS) and Branch-and-Bound (BB).** Classical CSP search procedures rely on recursive exploration of the search tree representing partial variable assignments. BTS is the foundational depth-first enumeration scheme for constraint satisfaction. At each recursive call, the current partial assignment  $\mathcal{A}_p$  is tested for consistency; if it violates a constraint, the search immediately backtracks (**fail**); if it assigns all variables consistently, the procedure terminates (**success**). Otherwise, an unassigned variable  $x_i$  is chosen, and the algorithm recursively expands all feasible value choices  $v \in \mathcal{D}(x_i)$ . This recursive process implicitly enumerates the feasible region defined by the constraints and forms the logical basis of many complete solvers.

---

**Algorithm 4 Depth-First Backtracking Search (BTS)**


---

```

(S04) Initialize partial assignment  $\mathcal{A}_p = \emptyset$ , constraint set  $\mathcal{C}$ , and variable ordering  $(x_1, \dots, x_n)$ .
(S14) If  $\mathcal{A}_p$  is total and satisfies all  $c_j \in \mathcal{C}$ , return success.
If  $\exists c_j \in \mathcal{C}$  such that  $\mathcal{A}_p(\text{scope}(c_j)) \notin c_j$ , return fail.
(S24) Select the next unassigned variable  $x_i$  and iterate over values  $v \in \mathcal{D}(x_i)$ :
    Add  $(x_i, v)$  to  $\mathcal{A}_p$  and recursively call DFS( $\mathcal{A}_p \cup \{(x_i, v)\}$ ).
    If a recursive call returns success, propagate upward.
    Otherwise, remove  $(x_i, v)$  and try the next  $v$ .
(S34) If all values in  $\mathcal{D}(x_i)$  fail, return fail.

```

---

The `success` and `fail` outcomes thus serve as Boolean indicators of feasibility propagation in the recursion: `success` marks a complete consistent solution, whereas `fail` indicates that no consistent extension of the current partial assignment exists. Backtracking ensures completeness but can grow exponentially in the number of variables, motivating the use of cost-based pruning. We discuss the `DFS` algorithm, below.

When an objective function  $f(x)$  is introduced, the same tree structure can be searched using the *branch-and-bound* strategy. Instead of exploring all feasible completions, branch-and-bound computes a lower bound  $f_{\min}(\mathcal{A}_p)$  (a valid lower bound on the objective value of all feasible completions of  $\mathcal{A}_p$ ) for each partial assignment. Any node whose bound exceeds the current incumbent  $f^*$  can be safely pruned. This converts pure feasibility search into an exact optimization scheme and forms the computational backbone of many mixed-integer and combinatorial solvers.

---

**Algorithm 5 Branch-and-Bound (BB)**


---

```

(S05) Initialize incumbent objective  $f^* = +\infty$ , root node representing the full
      feasible domain  $\mathcal{D}$ , and an empty search stack.

repeat
  (S15) Select a node  $\mathcal{A}_p$  from the stack (partial assignment). Compute a
        valid lower bound  $f_{\min}(\mathcal{A}_p)$  and check feasibility of  $\mathcal{A}_p$ .
  (S25) If  $\mathcal{A}_p$  is infeasible, discard the node (fail).
  If  $\mathcal{A}_p$  is complete and  $f(\mathcal{A}_p) < f^*$ , update  $f^* := f(\mathcal{A}_p)$  and record  $\mathcal{A}^* := \mathcal{A}_p$ 
    (success).
  (S35) Otherwise, if  $f_{\min}(\mathcal{A}_p) < f^*$ , branch on a variable  $x_i$  and push each
        subproblem  $\mathcal{A}_p \cup \{(x_i, v)\}$  for  $v \in \mathcal{D}(x_i)$  onto the stack.
  Prune any node with  $f_{\min}(\mathcal{A}_p) \geq f^*$ .
until stack is empty or optimal solution found.

```

---

In summary, Algorithm 4 provides the fundamental logical search mechanism, while Algorithm 5 extends it with numerical bounds to support optimization. Both can be viewed as discrete analogues of recursive dynamic programming, and their decision structure directly parallels the policy search mechanisms used later in reinforcement learning formulations.

**Breadth-First vs. Depth-First.** Let  $\text{depth}(\mathcal{A}_p)$  denote the number of assigned variables. Breadth-first search (BFS=Algorithm 6) explores nodes in increasing depth order, ensuring minimal-depth solutions but with exponential memory requirements. Depth-first search (DFS=Algorithm 7) explores along

a single branch until conflict, then backtracks. Modern solvers combine both strategies through iterative deepening or restarts, providing full coverage while controlling memory.

---

**Algorithm 6 Breadth-First Search (BFS)**


---

```
(S06) Given constraint set  $\mathcal{C}$  over variables  $(x_1, \dots, x_n)$ , initialize a queue  $Q \leftarrow [\mathcal{A}_0]$  with the empty assignment  $\mathcal{A}_0 = \emptyset$ .
repeat
  (S16) Dequeue the first node  $\mathcal{A}_p$  from  $Q$ .
  If  $\mathcal{A}_p$  is total and satisfies all  $c_j \in \mathcal{C}$ , return success.
  If  $\exists c_j \in \mathcal{C}$  such that  $\mathcal{A}_p(\text{scope}(c_j)) \notin c_j$ , skip to the next node.
  (S26) For the next unassigned variable  $x_i$ , generate child nodes  $\mathcal{A}'_p = \mathcal{A}_p \cup \{(x_i, v)\}$  for all  $v \in \mathcal{D}(x_i)$ , and enqueue each  $\mathcal{A}'_p$  into  $Q$ .
until  $Q$  is empty.
Return fail.
```

---



---

**Algorithm 7 Depth-First Search (DFS)**


---

```
(S07) Given constraint set  $\mathcal{C}$  over variables  $(x_1, \dots, x_n)$ , initialize a stack  $S \leftarrow [\mathcal{A}_0]$  with the empty assignment  $\mathcal{A}_0 = \emptyset$ .
repeat
  (S17) Pop the top node  $\mathcal{A}_p$  from  $S$ .
  If  $\mathcal{A}_p$  is total and satisfies all  $c_j \in \mathcal{C}$ , return success.
  If  $\exists c_j \in \mathcal{C}$  such that  $\mathcal{A}_p(\text{scope}(c_j)) \notin c_j$ , continue.
  (S27) Select the next unassigned variable  $x_i$ , generate child nodes  $\mathcal{A}'_p = \mathcal{A}_p \cup \{(x_i, v)\}$  for all  $v \in \mathcal{D}(x_i)$ , and push each  $\mathcal{A}'_p$  onto  $S$ .
until  $S$  is empty.
Return fail.
```

---

**Completeness and Termination.** All search algorithms described are complete for finite-domain CSPs, guaranteeing termination with either **success** or **fail**. However, in the absence of strong pruning or learned guidance, their expected time complexity remains exponential in  $|\mathcal{X}|$ , underscoring the importance of heuristic and ML-based acceleration.

Both algorithms enumerate the same search tree but in different traversal orders: **BFS** guarantees the shallowest solution first but requires large memory, whereas **DFS** uses minimal memory but may explore deep infeasible paths. Iterative deepening combines the advantages of both by bounding the recursion depth and gradually increasing the limit.

**Constraint Graph Representation.** Every CSP induces a constraint graph  $G = (V, E)$  with  $V = \mathcal{X}$  and  $(x_i, x_k) \in E$  if variables co-occur in some  $c_j$ . Search procedures can then be viewed as traversals of  $G$  guided by variable-ordering heuristics. For instance, the *minimum remaining values (MRV)* heuristic selects

$$x_i^* = \operatorname{argmin}_{x_i \in \mathcal{X} \setminus \operatorname{dom}(\mathcal{A}_p)} |\mathcal{D}(x_i)|$$

to reduce branching factor.

Beyond uninformed strategies such as BFS and DFS, heuristic-guided algorithms use cost estimates to prioritize promising partial assignments.

**A\* Search.** A\* is a classical best-first search algorithm combining path-cost accumulation with heuristic guidance. At each step, it expands the node minimizing  $f(s) = g(s) + h(s)$ , where  $g(s)$  is the known cost from the start state and  $h(s)$  is a heuristic estimate of the remaining cost to the goal. For each successor  $s'$  of state  $s$ ,  $c(s, s')$  denotes the transition cost between them. Under an admissible heuristic, A\* is both complete and optimal, serving as the foundation for many classical planning and constraint-search procedures. Algorithm 8 summarizes the standard A\* framework.

**From Classical Search to CDCL.** Modern SAT solvers extend classical CSP search through conflict-driven clause learning (CDCL), non-chronological backtracking, and restart strategies. These mechanisms augment Algorithm 4 with learned “nogoods” that prevent revisiting inconsistent subspaces. The way propagation, learning, and restart mechanisms reinforce one another provides the rationale for the ML-augmented CSP/SAT architectures developed later on.

---

**Algorithm 8 Classical A\* Search Algorithm**

---

**Initialization**

(S0<sub>8</sub>) Initialize the **open list** with the start node  $s_{\text{start}}$ ; set  $g(s_{\text{start}}) := 0$  and  $f(s_{\text{start}}) := h(s_{\text{start}})$ . Initialize the **closed list** as empty.

**repeat**

**Node Selection and Expansion**

(S1<sub>8</sub>) Select from the open list the node  $s$  with the smallest  $f(s) = g(s) + h(s)$ . If  $s$  is the goal state, terminate and reconstruct the path. Otherwise, remove  $s$  from the open list and add it to the closed list.

**Successor Generation**

(S2<sub>8</sub>) For each successor  $s'$  of  $s$  with transition cost  $c(s, s')$ :

- Compute tentative cost  $g'(s') = g(s) + c(s, s')$ .
- If  $s' \notin \text{open/closed lists}$  or  $g'(s') < g(s')$ , update:

$$g(s') := g'(s'), \quad f(s') := g(s') + h(s'),$$

and record  $s'$ 's parent as  $s$ .

- Add  $s'$  to the open list if not already present.

**Termination**

(S3<sub>8</sub>) Repeat (S1<sub>8</sub>)–(S2<sub>8</sub>) until the open list is empty (no solution) or a goal node is found. Return the path of minimal total cost  $f(s)$  if successful.

**until** goal reached or open list empty

---

We next present generic frameworks for both approaches. LCG (=Algorithm 9) illustrates the LCG procedure, which iteratively applies constraint propagation, heuristic decisions, and conflict analysis until either a satisfying assignment is found or infeasibility is proven.

---

**Algorithm 9 A Generic LCG Framework**


---

**Initialization**

(S0<sub>9</sub>) Initialize  $\mathcal{A}$ , decision level  $d$ , working set  $\mathcal{C}_{\text{working}}$ , record **trial**, and **conflict**.

**repeat**

**Constraint propagation**

(S1<sub>9</sub>) Reduce domains, assign forced values, and detect conflicts.

**Heuristic decision**

(S2<sub>9</sub>) If no conflict, select a variable, assign a value, increase decision level, and continue.

**Conflict analysis**

(S3<sub>9</sub>) If conflict, derive a learned clause, backjump, and resume. If  $d_{\text{backjump}} < 0$ , declare UNSAT.

**until** all clauses in  $\mathcal{C}_{\text{working}}$  are satisfied or a conflict is detected at the root level

---

**(S0<sub>9</sub>) Initialization.** The solver initializes the partial assignment  $\mathcal{A} := \emptyset$ , sets  $d := 0$ , and defines the working set of constraints  $\mathcal{C}_{\text{working}} := \mathcal{C}$ . It also maintains a record **trial** of pairs  $(l_i, d)$  for each assigned literal  $l_i$  (either  $x_i$  or  $\neg x_i$ ), and initializes a Boolean conflict indicator **conflict** := 0.

**(S1<sub>9</sub>) Constraint propagation.** For each constraint  $c_k \in \mathcal{C}$ , domains are reduced as

$$D'(x_i) = \{v \in \mathcal{D}(x_i) \mid c_k(x_i = v) \text{ holds under } \mathcal{A}\}.$$

If  $D'(x_i) = \emptyset$  for some  $x_i$ , then a conflict is detected (**conflict** := 1). If  $D'(x_i) = \{v\}$ , then the assignment  $x_i = v$  is forced, and the assignment set is updated by

$$\mathcal{A} := \mathcal{A} \cup \{l_i = \text{true}\}, \quad \text{trial} := \text{trial} \cup \{(l_i, d)\}.$$

Propagation continues until no further domain reductions are possible or a conflict arises.

**(S2<sub>9</sub>) Heuristic decision.** If no conflict was detected in (S1<sub>9</sub>), the solver selects an unassigned variable  $x_i$  and a value  $v \in D'(x_i)$  according to a branching heuristic. The assignment

$$l_i = (x_i = v)$$

is added to the current assignment, and the decision level is increased:

$$\mathcal{A} := \mathcal{A} \cup \{l_i\}, \quad d := d + 1, \quad \text{trial} := \text{trial} \cup \{(l_i, d)\}.$$

**(S3<sub>9</sub>) Conflict analysis and backjumping.** If a conflict is detected in (S1<sub>9</sub>), the solver derives a learned clause  $c_{\text{learned}}$  from the conflicting constraints and augments the working set

$$\mathcal{C}_{\text{working}} := \mathcal{C}_{\text{working}} \cup \{c_{\text{learned}}\}.$$

It then computes the backjump level by examining the decision levels of the literals appearing in the learned clause  $c_{\text{learned}}$ . For simplicity, we define

$$d_{\text{backjump}} := \max\{d_i \mid l_i \in c_{\text{learned}}\},$$

that is, the highest decision level among its literals. In practice, modern CDCL solvers exclude the unique implication point (UIP) literal and use the *second-highest* decision level to ensure correct non-chronological backtracking. All assignments made at levels higher than  $d_{\text{backjump}}$  are then removed:

$$\mathcal{A} := \mathcal{A} \setminus \{l_i \mid d_i > d_{\text{backjump}}\}, \quad d := d_{\text{backjump}}.$$

If  $d_{\text{backjump}} < 0$ , the solver declares the instance UNSAT; otherwise, propagation resumes from the updated level.

The loop (S1<sub>9</sub>)–(S3<sub>9</sub>) continues until  $\mathcal{C}_{\text{working}} = \emptyset$ , in which case a satisfying assignment has been found and the solver returns SAT. If instead a conflict is detected at the root level (i.e.,  $d_{\text{backjump}} < 0$ ) and no further backtracking is possible, the solver declares UNSAT.

**Termination states.** The solver therefore terminates in one of two possible states:

- SAT — a satisfying assignment  $\mathcal{A}$  has been found such that all constraints in  $\mathcal{C}_{\text{working}}$  are satisfied;
- UNSAT — the solver has proven that no assignment  $\mathcal{A}$  can satisfy all constraints, i.e., the instance is unsatisfiable.

These outcomes correspond to the classical decision problem formulation of Boolean satisfiability.

CDCL (=Algorithm 10) differs from LCG mainly in the propagation step, since CDCL works purely on Boolean formulas encoded in CNF, while LCG combines SAT solving with CSP propagation. The overall structure is similar: initialization (S0<sub>10</sub>), unit propagation (S1<sub>10</sub>), heuristic decision (S2<sub>10</sub>), and conflict analysis with backjumping (S3<sub>10</sub>).

---

**Algorithm 10 A Generic CDCL Framework**


---

**Initialization**

(S0<sub>10</sub>) Initialize  $\mathcal{A}$ , decision level  $d$ , working set  $\mathcal{C}_{\text{working}}$ , record **trial**, and **conflict**.

**repeat**

**Unit propagation**

(S1<sub>10</sub>) Perform unit clause propagation and detect conflicts.

**Heuristic decision**

(S2<sub>10</sub>) If no conflict, select a variable, assign a value, increase decision level, and continue.

**Conflict analysis**

(S3<sub>10</sub>) If conflict, learn a clause, backjump, and resume. If  $d_{\text{backjump}} < 0$ , declare UNSAT.

**until**  $\mathcal{C}_{\text{working}} = \emptyset$  % return SAT.

---

**(S0<sub>10</sub>) Initialization.** The solver starts with an empty assignment  $\mathcal{A} := \emptyset$ , decision level  $d := 0$ , and the working clause set  $\mathcal{C}_{\text{working}} := \mathcal{C} = \{c_1, c_2, \dots, c_m\}$ . A record **trial** stores assignments and their decision levels,  $(l_i, d)$ , where  $l_i$  is a literal. The conflict flag is initialized as **conflict** := 0.

**(S1<sub>10</sub>) Unit propagation and conflict detection.** For each clause  $c_j = (l_1 \vee l_2 \vee \dots \vee l_k)$ , check:

- If exactly one literal is unassigned under  $\mathcal{A}$  and all other  $k - 1$  literals are false, i.e.

$$|\{l_i \mid l_i \text{ unassigned under } \mathcal{A}\}| = 1, \quad |\{l_i \mid l_i = 0 \text{ under } \mathcal{A}\}| = k - 1,$$

then the unassigned literal must be set to true. The assignment set is updated by

$$\mathcal{A} := \mathcal{A} \cup \{l_i = \text{true}\}, \quad \text{trial} := \text{trial} \cup \{(l_i, d)\}.$$

- If all literals in a clause are false under  $\mathcal{A}$ , i.e.

$$|\{l_i \mid l_i = 0 \text{ under } \mathcal{A}\}| = k,$$

then the clause is falsified, a conflict is detected, and **conflict** := 1.

This process continues until no more unit clauses remain.

**(S2<sub>10</sub>) Heuristic decision.** If no conflict was found, the solver chooses an unassigned variable  $x_i$  using a heuristic, assigns it a Boolean value, and increments the decision level:

$$\mathcal{A} := \mathcal{A} \cup \{l_i\}, \quad d := d + 1, \quad \text{trial} := \text{trial} \cup \{(l_i, d)\}.$$

**(S3<sub>10</sub>) Conflict analysis and backjumping.** If a conflict occurs, the solver identifies a conflict clause  $c_{\text{conflict}}$  and uses resolution to derive a learned clause  $c_{\text{learned}}$ , which is added to the working set:

$$\mathcal{C}_{\text{working}} := \mathcal{C}_{\text{working}} \cup \{c_{\text{learned}}\}.$$

The solver then computes the backjump level

$$d_{\text{backjump}} := \max\{d_i \mid l_i \in c_{\text{learned}}\},$$

and removes all assignments at levels higher than  $d_{\text{backjump}}$ :

$$\mathcal{A} := \mathcal{A} \setminus \{l_i \mid d_i > d_{\text{backjump}}\}, \quad d := d_{\text{backjump}}.$$

If  $d_{\text{backjump}} < 0$ , the formula is declared **unsatisfiable**. Otherwise, the solver resumes propagation.

The loop (S1<sub>10</sub>)–(S3<sub>10</sub>) continues until  $\mathcal{C}_{\text{working}} = \emptyset$ , in which case the formula is satisfiable.

### 3.2 NNs as Enhancers for CSP Solvers

The propagation, heuristic decision, and conflict analysis phases of LCG (Algorithm 9)/CDCL (Algorithm 10) correspond to the steps where ML or RL modules can be embedded. Equations defining logistic regression, GNN updates, and MDPs are omitted here since they are defined in Section 1; references below link directly to those foundations.

**Step (S1<sub>9</sub>)/(S1<sub>10</sub>) of LCG/CDCL – Propagation.** Propagation uses ML-predicted backbone variables and RL-guided pruning policies (definitions of policy  $\pi_\theta$  and reward shaping follow Section 1). Algorithm 11 summarizes the augmented propagation procedure.

The integration of learned heuristics into the propagation stage is summarized in Algorithm 11. This module extends (S1<sub>9</sub>) and (S1<sub>10</sub>) by embedding ML-driven backbone estimation and RL-based pruning policies directly into the consistency enforcement phase. In (S0<sub>11</sub>), statistical features are extracted from the CNF to initialize the logistic model. In (S1<sub>11</sub>), a Monte Carlo refinement estimates variable confidence and fixes high-probability backbone literals before search. In (S2<sub>11</sub>), an RL policy learns to prune infeasible domains, improving propagation efficiency in LCG. Finally, (S3<sub>11</sub>) integrates both ML predictions and RL guidance into a unified propagation routine, reducing conflict depth and enabling faster convergence [34, 56].

---

**Algorithm 11** ML-Enhanced Propagation for (S1<sub>9</sub>)/(S1<sub>10</sub>) of LCG/CDCL

---

**Initialization**

(S0<sub>11</sub>) Extract CNF features and train or load a logistic model for backbone prediction.

**Backbone Estimation**

(S1<sub>11</sub>) Use Monte Carlo sampling to estimate variable confidence; fix literals with high backbone probability.

**RL-Guided Pruning**

(S2<sub>11</sub>) Model propagation as a decision process; apply a learned policy to prune infeasible domains.

**Integration**

(S3<sub>11</sub>) Combine ML and RL guidance to accelerate propagation and reduce conflicts.

---

**RL Formulation for Pruning.** This paragraph formulates propagation pruning as an MDP with states  $(\mathcal{A}_t, \mathcal{C}_{\text{working}}^t)$ , actions  $\{\text{fix}, \text{prune}\}$ , and reward  $r_t$ . It is implemented in Algorithm 11 (S2<sub>11</sub>, S3<sub>11</sub>).

The propagation process can be modeled as a Markov decision process (MDP)

$$\mathcal{M}_{\text{prop}} = (\mathcal{S}, \mathcal{A}, \Pr, R, \gamma),$$

where the state  $s_t \in \mathcal{S}$  encodes the solver's internal configuration, including the current partial assignment and the working clause set, and the action  $a_t \in \mathcal{A}$  corresponds to fixing or pruning a literal. Transitions follow the solver's propagation dynamics  $\Pr(s_{t+1} | s_t, a_t)$ , and the reward signal quantifies progress in constraint reduction, for example,

$$r_t = |\mathcal{C}_{\text{working}}^{t-1}| - |\mathcal{C}_{\text{working}}^t|,$$

which measures the decrease in the number of active clauses or conflicts.

Formally, the propagation phase defines

$$\begin{aligned} s_t &= (\mathcal{A}_t, \mathcal{C}_{\text{working}}^t), \\ a_t &\in \{\text{fix}(x_i = v), \text{prune}(x_i = v)\}, \end{aligned}$$

$\Pr(s_{t+1} | s_t, a_t)$  describes the solver's update dynamics,

$$R_t = |\mathcal{C}_{\text{working}}^{t-1}| - |\mathcal{C}_{\text{working}}^t|,$$

$\gamma \in (0, 1)$  is the discount factor.

The policy  $\pi_\phi(a_t | s_t)$ , parameterized by  $\phi$ , is trained using the PPO objective (defined by (1) in Section 2) to maximize the expected discounted return  $\mathbb{E}_{\pi_\phi}[\sum_t \gamma^t R_t]$ , thus guiding the solver to prune infeasible branches efficiently.

In practical implementations, the state representation  $s_t$  is constructed from compact solver statistics—such as the number of active clauses, mean LBD, and current decision depth—or from neural embeddings of the working clause set  $\mathcal{C}_{\text{working}}$  produced by a GNN encoder. The policy  $\pi_\phi(a_t \mid s_t)$ , parameterized by  $\phi$ , is trained using the PPO objective (defined by (1) in Section 2) to maximize the expected discounted return

$$\mathbb{E}_{\pi_\phi} \left[ \sum_t \gamma^t r_t \right],$$

thereby learning an adaptive pruning strategy as formalized in Algorithm 11.

**Step (S2<sub>9</sub>)/ (S2<sub>10</sub>) of LCG/CDCL – Heuristic Decision.** Branching decisions use instance classification, parameter tuning, and policy optimization via PPO as described in Section 1. Equation-based definitions of classifiers and softmax predictors are omitted and replaced by references. Algorithm 12 summarizes the decision mechanism.

ML and RL enhance the heuristic decision phase by replacing static branching rules with adaptive, data-driven policies. Algorithm 12 extends (S2<sub>9</sub>) and (S2<sub>10</sub>) through instance classification, parameter tuning, and neural branching strategies. In (S0<sub>12</sub>), CNF features are collected and classified to select solver-specific configurations. In (S1<sub>12</sub>), parameters such as restart intervals and clause deletion thresholds are automatically tuned using learned performance models. In (S2<sub>12</sub>), branching variables are chosen through multi-armed bandit learning or transformer-based scoring, integrating polarity prediction for conflict reduction. Finally, (S3<sub>12</sub>) combines these models into an adaptive decision module that guides search direction and branching depth dynamically, achieving faster convergence and improved solver generalization [9, 15, 31, 47, 56].

**Step (S3<sub>9</sub>)/ (S3<sub>10</sub>) of LCG/CDCL – Conflict Analysis and Backjumping.** Conflict resolution benefits from ML-based clause utility prediction and RL-guided restart scheduling (as in the PPO framework introduced earlier). Algorithm 13 details the procedure.

ML further refines the conflict analysis and backjumping phase by predicting clause utility, guiding restart decisions, and prioritizing search in specialized domains. Algorithm 13 extends (S3<sub>9</sub>) and (S3<sub>10</sub>) through clause-utility prediction, RL-driven restart scheduling, and neural-guided search in cryptanalytic problems. In (S0<sub>13</sub>), clause statistics such as size, age, and LBD are collected after each conflict. In (S1<sub>13</sub>), a regression or neural model predicts the usefulness of learned clauses, allowing low-utility clauses to be deprioritized or removed. In (S2<sub>13</sub>), RL agents dynamically determine restart or continuation actions based on solver states, improving restart efficiency and clause quality. In

---

**Algorithm 12** ML-Enhanced Heuristic Decision for (S2<sub>9</sub>)/(S2<sub>10</sub>) of LCG/CDCL

---

**Initialization**

(S0<sub>12</sub>) Extract CNF features and classify instance type to load solver configuration and parameter settings.

**Parameter Optimization**

(S1<sub>12</sub>) Use learned performance models to adjust solver parameters (e.g., restart interval, clause deletion ratio) before search.

**Learning-Based Branching**

(S2<sub>12</sub>) Select branching variables using learning-rate-based multi-armed bandits or Transformer-based scoring via the attention formulation (defined by (6) in Section 2). Predict polarity using a classifier or logistic model (defined by (8) in Section 2) to align initial assignments with backbone tendencies.

**Integration and Result**

(S3<sub>12</sub>) Integrate classification, parameter tuning, and neural branching into the decision phase to guide variable selection dynamically while reducing conflicts. Achieves improved solver adaptability and faster convergence [9, 15, 31, 47, 56].

---

(S3<sub>13</sub>), domain-specific neural prioritization models, such as NeuroGIFT, adapt the solver’s backtracking strategy for cryptanalysis, ranking candidate assignments by plausibility. This combination of predictive and adaptive control significantly reduces redundant conflicts and enhances solver robustness [31, 34, 51].

**Literal Block Distance (LBD).** This paragraph defines the LBD metric for evaluating clause quality during conflict learning. It is employed in Algorithm 13 (S0<sub>13</sub>, S1<sub>13</sub>) to guide clause retention.

The Literal Block Distance (LBD) [3] is a clause-quality metric used in modern CDCL solvers to evaluate the relevance of learned clauses during conflict analysis. Let  $C = (l_1 \vee l_2 \vee \dots \vee l_k)$  be a learned clause, and let  $\text{level}(l_i)$  denote the decision level at which literal  $l_i$  was assigned. The LBD of clause  $C$  is defined as

$$\text{LBD}(C) = |\{\text{level}(l_i) \mid l_i \in C\}|,$$

that is, the number of distinct decision levels among the literals of  $C$ . Clauses with lower LBD values are considered more general and therefore more useful, since they connect fewer decision levels and tend to prune the search space more effectively. Consequently, LBD serves as a key heuristic for clause activity, retention, and deletion in high-performance solvers such as `Glucose` and `Kissat`.

**RL Formulation for Restart Scheduling.** This paragraph defines restart scheduling as an MDP over solver statistics with actions `{restart, continue}`

---

**Algorithm 13** ML-Enhanced Conflict Analysis and Backjumping for (S3<sub>9</sub>)/(S3<sub>10</sub>) of LCG/CDCL

---

**Initialization**

(S0<sub>13</sub>) Collect features of learned clauses (e.g., size, LBD, activity, age) after each conflict.

**Clause Utility Prediction**

(S1<sub>13</sub>) Use a regression or neural model to estimate clause utility. Retain high-utility clauses and remove or deprioritize those predicted to be less useful.

**RL-Guided Restart Scheduling**

(S2<sub>13</sub>) Represent the solver state as a decision process with actions {restart, continue}. Train an RL policy using the PPO objective (defined by (1) in Section 2) to maximize runtime efficiency by selecting optimal restart moments based on conflict patterns.

**Neural Prioritization and Integration**

(S3<sub>13</sub>) Integrate domain-specific models such as NeuroGIFT to prioritize search branches or candidate assignments using neural scoring. Combine predictions with a restart policy for adaptive backjumping and faster convergence.

**Result**

ML models improve clause retention and restart scheduling, while neural prioritization accelerates key recovery and structured search [31, 34, 51].

---

and reward based on conflict reduction. It is used in Algorithm 13 (S2<sub>13</sub>, S3<sub>13</sub>).

Restart scheduling can be modeled as a Markov decision process (MDP)

$$\mathcal{M}_{\text{restart}} = (\mathcal{S}, \mathcal{A}, \text{Pr}, R, \gamma),$$

where the state  $s_t \in \mathcal{S}$  encodes solver statistics such as the current number of conflicts, the mean LBD value  $\overline{\text{LBD}}_t$ , and the current decision level  $d_t$ . The available actions are  $a_t \in \{\text{restart}, \text{continue}\}$ , and transitions follow the solver's internal update dynamics  $\text{Pr}(s_{t+1} | s_t, a_t)$ . The reward encourages reductions in the conflict rate:

$$r_t = \Delta_{\text{conflict}}^{t-1} - \Delta_{\text{conflict}}^t,$$

where  $\Delta_{\text{conflict}}^t$  denotes the average number of conflicts per decision window. A policy  $\pi_\phi(a_t | s_t)$ , parameterized by  $\phi$ , is trained using the PPO objective (defined by (1) in Section 2) to maximize the expected discounted return

$$\mathbb{E}_{\pi_\phi} \left[ \sum_t \gamma^t r_t \right],$$

thereby providing an adaptive mechanism for determining optimal restart points based on real-time solver behavior.

**Neural Prioritization Model (NeuroGIFT).** This paragraph describes NeuroGIFT, a neural encoder–decoder framework that ranks candidate assignments for cryptanalytic SAT solving. It is implemented in Algorithm 13 (S3<sub>13</sub>).

NeuroGIFT employs a neural encoder–decoder architecture to prioritize candidate assignments during cryptanalytic search. The encoder maps the variable–clause adjacency matrix into hidden embeddings, while the decoder produces a ranked list of promising variable assignments that are fed back into the solver as branching priorities. Input features represent Boolean variables and clause dependencies, which are processed through multilayer perceptrons to yield scores indicating assignment likelihood. These scores are iteratively refined using feedback from solver conflicts, integrating neural ranking with traditional CDCL backjumping. This hybrid design enables adaptive prioritization while preserving solver soundness.

**Beyond the Core Loop.** This paragraph discusses ML for analyzing SAT community structures and learning interpretable decision trees using SAT encodings. It is applied in Algorithm 14 (S0<sub>14</sub>–S3<sub>14</sub>).

ML has also been used to study the structure of SAT formulas themselves. Community-structured SAT formulas exhibit thresholds different from random SAT, and ML-based analysis has been instrumental in understanding satisfiability phase transitions in such structured cases [6]. Furthermore, SAT solving itself can serve ML: for instance, SAT encodings have been developed for learning *optimal decision trees*, yielding compact, interpretable models that contribute explainable AI [37].

Beyond the core solving loop, ML contributes to structural analysis and interpretable model construction. Algorithm 14 extends this perspective by incorporating ML-based structural study and SAT-encoded model learning. In (S0<sub>14</sub>), the solver extracts graph-level and community-based statistics from SAT instances to characterize problem structure. In (S1<sub>14</sub>), these representations are used to identify community organization and predict phase transition regions. In (S2<sub>14</sub>), SAT-based encodings are employed to learn interpretable models such as optimal decision trees. Finally, (S3<sub>14</sub>) integrates these insights to guide both solver analysis and the synthesis of explainable ML models [6, 37].

**Community Structure Metrics.** This paragraph defines modularity  $Q$  as a measure of community structure in SAT clause–variable graphs. It is employed in Algorithm 14 (S1<sub>14</sub>).

Given a CNF formula  $\phi$ , let  $\mathcal{G} = (V_{\text{var}} \cup V_{\text{cl}}, E)$  denote its bipartite clause–variable graph, where  $V_{\text{var}}$  and  $V_{\text{cl}}$  represent variable and clause nodes, respectively. The

---

**Algorithm 14** ML Applications Beyond the Core Loop of LCG/CDCL

---

**Initialization**

(S0<sub>14</sub>) Collect global CNF features and construct a clause–variable or community graph representation.

**Structural Analysis**

(S1<sub>14</sub>) Use ML models to detect community structures and estimate satisfiability thresholds in complex SAT instances.

**SAT-Encoded Learning**

(S2<sub>14</sub>) Encode interpretable models such as optimal decision trees as CNF formulas and solve them using SAT to obtain minimal, consistent models.

**Integration and Result**

(S3<sub>14</sub>) Combine structural insight with SAT-encoded model learning to enhance solver analysis and contribute explainable, hybrid neuro-symbolic reasoning frameworks [6, 37].

---

community structure of  $\mathcal{G}$  is quantified by the modularity measure

$$Q = \frac{1}{2|E|} \sum_{i,j} \left[ A_{ij} - \frac{k_i k_j}{2|E|} \right] \delta(c_i, c_j),$$

where  $A_{ij}$  is the adjacency matrix,  $k_i$  is the degree of node  $i$ ,  $c_i$  its community label, and  $\delta(\cdot, \cdot)$  is the Kronecker delta. For simplicity, the clause–variable bipartite graph is treated as undirected when computing the modularity  $Q$ . For bipartite graphs  $\mathcal{G}$ , node degrees are normalized such that  $\sum_i k_i = 2|E|$ , ensuring that the modularity  $Q$  remains properly scaled under the clause–variable partition. ML models leverage  $Q$  and related graph-structural features to predict satisfiability thresholds and phase-transition behavior in structured SAT instances.

**SAT-Encoded Optimal Decision Trees.** This paragraph presents SAT-encoded optimal decision-tree learning, ensuring logical consistency between sample labels and tree paths. It is used in Algorithm 14 (S2<sub>14</sub>, S3<sub>14</sub>).

Learning an optimal decision tree of depth  $d$  can be formulated as a SAT problem. Each internal node corresponds to a Boolean variable  $z_j$  representing a split predicate, and each leaf encodes a class label  $y_\ell$ . For a dataset  $\{(x_i, y_i)\}_{i=1}^N$ , the CNF encoding enforces label consistency between samples and tree structure as

$$\bigwedge_{i=1}^N \bigvee_{\ell \in L} \left( (x_i \models \text{path}(\ell)) \rightarrow (y_i = y_\ell) \right),$$

where each  $\text{path}(\ell)$  represents a conjunction of split predicates leading to leaf  $\ell$

with class label  $y_\ell$ . Equivalently, the constraint can be expressed as

$$y_i = f_{\text{tree}}(x_i; z_1, \dots, z_d), \quad \forall i \in [N],$$

where  $f_{\text{tree}}$  is the Boolean function realized by the candidate tree. Solving the resulting CNF yields a tree of minimal size that satisfies all label constraints, thereby producing an interpretable, globally optimal classifier learned through logical inference.

**Neural Architectures for SAT Solving.** Neural architectures for SAT solving extend the graph-based and attention-based foundations established in Section 1. Given a clause–literal bipartite graph  $\mathcal{G} = (V_{\text{lit}} \cup V_{\text{cl}}, E)$  representing a Boolean formula in CNF, each literal  $v \in V_{\text{lit}}$  and clause  $c \in V_{\text{cl}}$  is assigned an embedding  $h_v, h_c \in \mathbb{R}^d$  that is iteratively refined through message passing (defined by Eq. (4) in Section 2). The following neural models specialize this formulation:

- **NeuroSAT** [46] formulates satisfiability prediction as a binary classification problem over the entire clause–literal graph. At each iteration  $k$ , literal and clause embeddings are updated by

$$h_c^{(k+1)} = \text{MLP}_c \left( \sum_{v \in N(c)} h_v^{(k)} \right), \quad h_v^{(k+1)} = \text{MLP}_v \left( h_v^{(k)}, \sum_{c \in N(v)} h_c^{(k+1)} \right),$$

followed by a graph-level pooling  $\hat{y} = \sigma(\mathbf{w}^\top \sum_v h_v^{(K)})$  that predicts whether the formula is satisfiable.

- **NeuralsAT** [45] extends this idea by coupling unsatisfiable-core prediction with clause-level attention. For each clause embedding  $h_c^{(K)}$ , an attention score  $\alpha_c = \text{softmax}(\mathbf{q}^\top h_c^{(K)})$  estimates its likelihood of belonging to an unsat core. The network minimizes a cross-entropy loss  $L_{\text{unsat}} = -\sum_c [y_c \log \alpha_c + (1 - y_c) \log(1 - \alpha_c)]$ , guiding solver heuristics such as clause deletion and restart policies.
- **SATFormer** [48] replaces local message passing with global multi-head attention (defined by Eqs. (6)–(7) in Section 2) applied to tokenized clause–literal embeddings. The model computes  $\text{Attn}(Q, K, V) = \text{softmax}(QK^\top / \sqrt{d_k})V$  over all variable–clause pairs, enabling long-range relational reasoning. A transformer decoder then produces satisfiability logits or variable activity scores used for branching and clause ranking.

### 3.3 Software using LCG and CDCL algorithms

**Lazy Clause Generation (LCG)-based Solvers.** LCG-based solvers integrate the propagation mechanisms of finite-domain constraint programming (CP) with the learning capabilities of Boolean satisfiability (SAT) solvers, combining expressive high-level modeling with efficient conflict-driven search. Among state-of-the-art LCG systems, **Chuffed** [50] is a solver designed from the ground up around the principles of lazy clause generation. Each finite-domain propagator in **Chuffed** records the reasons for its propagations as implication clauses, constructing a conflict graph similar to that of CDCL SAT solvers. This enables the derivation of *nogoods*, non-chronological backjumping, and variable activity heuristics based on the VSIDS scheme, achieving substantial reductions in redundant search while maintaining tight integration between the SAT and CP layers.

**ECLiPSe** [2] provides a foundational constraint logic programming (CLP) environment that has strongly influenced the architecture of modern LCG solvers. Developed as a research and industrial platform for constraint-based modeling, it supports hybrid solvers for integer, real, and Boolean domains, an open module system for defining new propagators, and a robust language interface to external solvers. Its design philosophy—separating modeling, search control, and solver implementation—continues to inform LCG system architecture.

**Gecode** [44] represents a highly optimized and extensible C++ library for constraint programming. It offers an extensive collection of global constraints, advanced propagation algorithms, customizable search strategies, and efficient multi-core parallel search engines. As an open-source framework under the MIT license, **Gecode** has become a reference implementation for academic research and a back-end for modeling languages such as **Minizinc**. Its modular kernel allows the rapid development and testing of new propagation algorithms and branching heuristics, making it an essential component in the evolution of hybrid CP--SAT technologies.

Finally, **Picat** [59] is a modern logic-based multi-paradigm language that unifies logic, functional, constraint, and imperative programming. Its built-in constraint modules (`cp`, `sat`, `mip`, and `smt`) provide a unified interface to multiple solving paradigms, allowing the seamless application of SAT-based encodings within a declarative modeling environment. The **PicatSAT** compiler integrates LCG-style clause learning with high-level constraint representations, while its tabling and dynamic programming features extend the solver’s capabilities to planning and optimization problems. Together, these solvers—from **ECLiPSe**’s CLP foundations to **Gecode**’s extensible architecture, **Chuffed**’s hybrid clause learning, and **Picat**’s declarative multi-paradigm integration—illustrate the continuous convergence of CP and SAT paradigms that defines the modern LCG landscape.

**Conflict-Driven Clause Learning (CDCL)-based Solvers.** CDCL-based solvers form the core of modern propositional and satisfiability modulo theories (SMT) solving. They extend the classical DPLL procedure with conflict-driven clause learning, non-chronological backjumping, restarts, and variable activity heuristics. Among the most influential solvers in this lineage, **MiniSAT** [18] stands as a minimalist yet extensible implementation that crystallized the modern CDCL architecture. It introduced efficient data structures such as watched literals for Boolean constraint propagation and offered a clean C++ interface, allowing it to serve as a foundation for later high-performance solvers. **Glucose** [3], derived from **MiniSAT**, pioneered the use of the LBD (Literal Blocks Distance) metric to evaluate the quality of learnt clauses, introducing the concept of “glue clauses” that connect fewer decision levels and thus contribute most effectively to pruning the search space. This innovation led to predictive clause management strategies that became standard across subsequent solvers.

**PicoSAT** [10] emphasized low-level performance optimization through memory-efficient occurrence lists and aggressive restart policies. Its innovations in data layout and proof trace compression improved both runtime and proof generation efficiency, establishing new baselines for solver engineering. **MapleSAT** [32] integrated machine learning concepts into branching heuristics via the **Learning Rate Branching** (LRB) algorithm, viewing variable selection as an online optimization process inspired by reinforcement learning. This approach significantly improved solver adaptability across heterogeneous benchmark categories.

**Kissat** [11], a recent descendant of **CaDiCaL**, exemplifies a modern high-performance CDCL solver engineered for simplicity, determinism, and cache efficiency. Written in C, it combines optimized restarts, inprocessing, and lightweight preprocessing while maintaining the lean structure of **MiniSAT**. **CryptoMiniSAT** [49] extends the CDCL framework to cryptographic reasoning by adding native **XOR** constraint propagation through Gaussian elimination, enabling efficient treatment of algebraic relations in cryptanalysis problems.

Beyond pure SAT solving, **Z3** [16] and **Yices** [17] extend CDCL into the domain of SMT solving. **Z3** integrates Boolean reasoning with first-order theories such as arithmetic and arrays via the DPLL(T) architecture, providing a powerful platform for verification, synthesis, and symbolic reasoning. Similarly, **Yices** combines a DPLL-based Boolean core with specialized theory solvers for arithmetic, arrays, bit-vectors, and uninterpreted functions, supporting MAX-SMT, unsat-core extraction, and model construction. Both solvers implement flexible APIs and serve as backends in major formal verification environments, including **PVS** and **SAL**. Together, these CDCL-based solvers—spanning from **MiniSAT**’s modular foundation to **Kissat**’s streamlined engineering, **Glucose**’s clause-quality learning, **MapleSAT**’s machine-learning heuristics, and **Z3/Yices**’s theory integration—define the state-of-the-art in SAT and SMT solving technology.

## 4 Direct Solution Learning for CSPs

Direct solution learning aims to construct models that can infer satisfying assignments for CSPs without relying on explicit symbolic search or iterative propagation. Instead of exploring the search tree step by step, these models learn to approximate the solution operator—a mapping from problem instances to feasible solutions—through data-driven generalization.

The goal of this section is to formalize how learning algorithms can replace the traditional search process with direct prediction. The central intuition is that by exposing a model to many solved instances, it can internalize the structural regularities that govern feasible assignments and thus infer new solutions in a single forward pass. This perspective reframes constraint solving as a supervised or self-supervised task: instead of discovering a solution through combinatorial reasoning, the system learns the function that generates it.

Understanding direct solution learning is crucial because it represents the most aggressive form of learning integration into constraint satisfaction problems: the solver itself becomes a trained model. Such systems outline a path toward amortized inference, rapid decoding of structured solutions, and hybrid solvers that combine symbolic consistency checks with fast parametric prediction, ultimately expanding the design space for efficient problem-solving architectures.

### 4.1 Technical Formulation of the Solution Operator

These models approximate the *solution operator*

$$\Phi : \mathcal{I} \rightarrow \mathcal{S}, \quad \Phi(I) = \mathcal{A}_I \text{ such that } \mathcal{A}_I \models \mathcal{C}_{\text{working}}(I),$$

where  $\mathcal{I}$  denotes the space of encoded CSP instances,  $\mathcal{S}$  the space of feasible assignments, and  $\mathcal{C}_{\text{working}}$  the active constraint set during inference. Here,  $\mathcal{A}_I : \mathcal{X} \rightarrow \mathcal{D}$  is a predicted assignment that satisfies the active constraint set  $\mathcal{C}_{\text{working}}(I)$ . This formulation parallels the satisfiability operator used in classical search, but replaces discrete branching with parametric inference.

### 4.2 Supervised and Self-Supervised Learning for CSP

Given a dataset

$$\mathcal{D}_{\text{CSP}} = \{(I_i, \mathcal{A}_i)\}_{i=1}^N,$$

each  $I_i$  is an encoded instance, and  $\mathcal{A}_i$  is a known feasible assignment satisfying all constraints in  $\mathcal{C}_{\text{working}}(I_i)$ . A parametric model  $f_\theta : \mathcal{I} \rightarrow \mathcal{S}$  is trained to

minimize

$$L(\theta) = \frac{1}{N} \sum_{i=1}^N \ell(f_\theta(I_i), \mathcal{A}_i) + \lambda \sum_{C \in \mathcal{C}_{\text{working}}(I_i)} \mathbb{I}[\neg(\mathcal{A}_i \models C)],$$

where  $\ell(\cdot, \cdot)$  measures assignment distance (e.g., mean-squared error or cross-entropy),  $\lambda > 0$  penalizes constraint violations, and  $\mathbb{I}$  is the indicator function. The model's prediction  $\hat{\mathcal{A}}_i = f_\theta(I_i)$  approximates the satisfying assignment for instance  $I_i$ .

**Self-Supervised Constraint Optimization.** When labeled assignments  $\mathcal{A}_i$  are unavailable, training uses constraint-driven self-supervision. Each constraint  $C_j(x_{S_j})$  defines a relaxable satisfaction function  $\psi_j(x_{S_j}) \in [0, 1]$ . The objective maximizes expected satisfaction:

$$\max_{\theta} \mathbb{E}_{I \sim \mathcal{D}_{\text{unsup}}} \left[ \frac{1}{|\mathcal{C}_{\text{working}}(I)|} \sum_{C_j \in \mathcal{C}_{\text{working}}(I)} \psi_j(f_\theta(I)_{S_j}) \right].$$

This constraint-aware objective aligns with the self-supervised principles used for backbone and polarity estimation.

To ensure discrete feasibility, a differentiable binarization layer  $\rho_\tau(z) = \text{sigmoid}(z/\tau)$  with temperature  $\tau > 0$  enforces near-binary variable values:

$$\hat{x}_i = \rho_\tau(z_i), \quad z_i \in \mathbb{R},$$

allowing end-to-end gradient flow while approximating integral assignments.

**Graph Encoding and GNN Message Passing.** Each CSP instance is represented by a bipartite graph  $G = (V_X \cup V_C, E)$ , connecting variable nodes  $V_X$  and constraint nodes  $V_C$ . The GNN update rule (consistent with Eq. (4), defined in Section 2) is

$$h_v^{(k+1)} = \phi_{\text{upd}} \left( h_v^{(k)}, \sum_{u \in \mathcal{N}(v)} \phi_{\text{msg}}(h_u^{(k)}, e_{uv}) \right),$$

where  $\mathcal{N}(v)$  is the neighborhood of  $v$  and  $\phi_{\text{upd}}$ ,  $\phi_{\text{msg}}$  are neural update functions. Final embeddings  $\{h_v^{(K)}\}$  are decoded by  $g_\theta$  to produce variable assignments  $\hat{x}_i$ . This representation mirrors the clause–literal graphs used in SAT-based neural solvers.

### 4.3 End-to-End Neural Solvers

End-to-end neural solvers embed both variable representation and constraint enforcement into a differentiable graph. Given an instance  $I = (\mathcal{X}, \mathcal{C}_{\text{working}})$ ,

$$z = \text{Enc}_\theta(I), \quad \hat{\mathcal{A}} = \text{Dec}_\phi(z),$$

where  $\text{Enc}_\theta$  is a GNN or Transformer encoder, and  $\text{Dec}_\phi$  predicts assignments  $\hat{\mathcal{A}} = (\hat{x}_1, \dots, \hat{x}_n)$ . Constraint satisfaction is measured by

$$R(I, \hat{\mathcal{A}}) = \frac{1}{|\mathcal{C}_{\text{working}}(I)|} \sum_{C_j \in \mathcal{C}_{\text{working}}(I)} \psi_j(\hat{\mathcal{A}}_{S_j}),$$

which parallels the RL reward design used for propagation and restart scheduling.

**Constraint Projection and Feasibility Refinement.** Predictions are refined by a differentiable projection operator:

$$\hat{\mathcal{A}}^{(t+1)} = \hat{\mathcal{A}}^{(t)} - \eta \nabla_{\hat{\mathcal{A}}} L_{\mathcal{C}_{\text{working}}}(\hat{\mathcal{A}}^{(t)}), \quad L_{\mathcal{C}_{\text{working}}}(\hat{\mathcal{A}}) = \sum_{C_j \in \mathcal{C}_{\text{working}}(I)} [1 - \psi_j(\hat{\mathcal{A}}_{S_j})]^2,$$

where  $\eta > 0$  is a step size. This mirrors conflict-resolution updates in LCG/CDCL, ensuring projection-based satisfaction rather than symbolic clause learning.

**Sequential Policy Formulation.** Alternatively, direct solving can be cast as a sequential decision policy  $\pi_\phi(a_t | s_t)$  generating partial assignments:

$$s_t = (\mathcal{A}_t, \mathcal{C}_{\text{working}}^t), \quad a_t \in \{\text{assign}, \text{backtrack}\}.$$

Rewards follow the reduction in unsatisfied constraints:

$$r_t = |\mathcal{C}_{\text{working}}^{t-1}| - |\mathcal{C}_{\text{working}}^t|,$$

and  $\pi_\phi$  is optimized by the PPO objective (defined by (1) in Section 2). This MDP formalism is identical to that used for propagation pruning in Algorithm 11.

### 4.4 Transfer and Meta-Learning across CSP Families

When CSP instances arise from similar distributions, learned solvers can transfer knowledge. Given source and target families  $(\mathcal{F}_{\text{src}}, \mathcal{F}_{\text{tgt}})$ , adaptation minimizes

$$\min_{\theta'} \mathbb{E}_{I \sim \mathcal{F}_{\text{tgt}}} L(f_{\theta'}(I), \mathcal{A}_I) \quad \text{s.t.} \quad \|\theta' - \theta\|_2^2 \leq \epsilon,$$

with  $\epsilon > 0$  bounding deviation from pretrained weights  $\theta$ . Meta-learning further optimizes for fast adaptation:

$$\theta'_k = \theta - \alpha \nabla_{\theta} L_{\mathcal{F}_k}(\theta), \quad \min_{\theta} \sum_k L_{\mathcal{F}_k}(\theta'_k),$$

where  $\alpha > 0$  is the inner learning rate.

**Cross-Domain Generalization.** Constraint-aware, binarized networks [29] generalize across structured CSP types (scheduling, resource allocation, etc.) by training on mixed distributions using shared encoders and consistency losses.

In summary, direct solution learning reinterprets CSP solving as differentiable constraint satisfaction:

$$I \xrightarrow{f_{\theta}} \hat{\mathcal{A}} \xrightarrow{\Pi_{\mathcal{C}_{\text{working}}}} \mathcal{A}^*,$$

where  $f_{\theta}$  produces a candidate assignment and  $\Pi_{\mathcal{C}_{\text{working}}}$  ensures feasibility.

## 5 Learning Algorithms for Heuristic Search

Both heuristics guide branching by exploiting information gathered during conflicts, yet they emphasize different signals. The **VSIDS** strategy in Algorithm 15 promotes variables that frequently occur in learned clauses and applies multiplicative decay to emphasize recent activity, allowing the search to follow emerging conflict patterns. In contrast, the **CHB** strategy in Algorithm 16 increases the score of variables whose assignments have directly contributed to resolving conflicts, capturing their historical effectiveness. Together, Algorithms 15 and 16 illustrate two complementary approaches to steering heuristic search: one driven by clause-based activity and the other by conflict-resolution history.

---

**Algorithm 15 Variable State Independent Decaying Sum (VSIDS) Heuristic**

---

**Initialization**

(S0<sub>15</sub>) Initialize all variable scores to zero:  $\text{score}(x_i) \leftarrow 0$  for all  $x_i \in \mathcal{X}$ .

**Score Update**

(S1<sub>15</sub>) Each time a new clause  $C_{\text{learned}}$  is learned, increment the score of each variable appearing in the clause:  $\text{score}(x_i) \leftarrow \text{score}(x_i) + 1$  for all  $x_i \in C_{\text{learned}}$ .

**Decay Step**

(S2<sub>15</sub>) Periodically decay all scores using a multiplicative decay factor  $\beta \in (0, 1)$  (typically  $\beta = 0.95$ ):  $\text{score}(x_i) \leftarrow \beta \cdot \text{score}(x_i)$  for all  $x_i \in \mathcal{X}$ .

**Variable Selection**

(S3<sub>15</sub>) Select the next branching variable as the unassigned variable with the maximum score:

$$x^* = \underset{x_i \in \mathcal{X}_{\text{unassigned}}}{\text{argmax}} \text{score}(x_i).$$

**Assignment Phase**

(S4<sub>15</sub>) Assign  $x^*$  using polarity caching, reusing its last successful truth value. If no prior polarity is available, assign randomly or using a default heuristic.

**Iteration**

(S5<sub>15</sub>) Repeat steps (S1<sub>15</sub>)–(S4<sub>15</sub>) throughout the solver loop, allowing the scores to evolve dynamically as new clauses are learned and conflicts are resolved.

---

---

**Algorithm 16 Conflict History Based (CHB) Heuristic**

---

**Initialization**

(S0<sub>16</sub>) Initialize an effectiveness counter for each variable:  $\text{eff}(x_i) \leftarrow 0$  for all  $x_i \in \mathcal{X}$ .

**Conflict Tracking**

(S1<sub>16</sub>) During search, record whether assigning a variable  $x_i$  contributes to resolving a conflict. Maintain a per-variable history of effectiveness events.

**Reward Update**

(S2<sub>16</sub>) Each time the assignment of  $x_i$  helps resolve a conflict, increase its effectiveness counter:  $\text{eff}(x_i) \leftarrow \text{eff}(x_i) + 1$ .

**Variable Selection**

(S3<sub>16</sub>) Select the next branching variable as the unassigned variable with the highest effectiveness score:

$$x^* = \underset{x_i \in \mathcal{X}_{\text{unassigned}}}{\operatorname{argmax}} \text{eff}(x_i).$$

**Assignment Phase**

(S4<sub>16</sub>) Assign the chosen variable  $x^*$  using polarity caching as in the VSIDS heuristic (Algorithm 15), reusing its last successful truth value.

**Iteration**

(S5<sub>16</sub>) Repeat the process as conflicts are detected and resolved, allowing the effectiveness counters to evolve adaptively during search.

---

## 6 Network Flow

This section provides full mathematical formulations for the classical network-flow and graph-optimization problems. Each model is presented with its objective, constraints, and variable definitions, together with optional diagrams illustrating graph structure.

**Traffic Routing Optimization (TRO).** The TRO problem [39] with quality-of-service (QoS) guarantees aims to determine optimal routing strategies that minimize overall network latency or maximize throughput while satisfying QoS constraints such as bandwidth, delay, and jitter.

Let the network be represented by a directed graph  $G = (V, L)$ , where  $V$  is the set of nodes and  $L$  is the set of directed links (or edges). Each link  $l \in L$  has an associated latency (or delay) cost function  $c_l(x_l)$  that depends on the flow  $x_l$  traversing it, and a capacity limit  $u_l > 0$  specifying the maximum allowable flow. Denote by  $P$  the set of all admissible paths in the network, where  $P_l \subseteq P$  is the subset of paths that include link  $l$ , and by  $P_{\text{in}}(v)$  and  $P_{\text{out}}(v)$  the sets of paths entering and exiting node  $v \in V$ , respectively. The goal is to minimize the total network cost:

$$\min_x \sum_{l \in L} c_l(x_l),$$

subject to flow conservation and link capacity constraints.

The TRO problem can be formulated as:

$$\begin{aligned} \min & \quad \sum_{l \in L} c_l(x_l) \\ \text{s.t.} & \quad \sum_{p \in P_{\text{in}}(v)} x_p - \sum_{p \in P_{\text{out}}(v)} x_p = 0, \quad \forall v \in V, \\ & \quad \sum_{p \in P_l} x_p \leq u_l, \quad \forall l \in L, \\ & \quad x_p \in s_p \mathbb{Z}_+, \quad \forall p \in P, \end{aligned} \tag{11}$$

where  $x_l$  is the total flow on link  $l$ ,  $x_p$  is the flow assigned to path  $p$ ,  $c_l(x_l)$  is a nonlinear latency or congestion cost function (often convex and increasing),  $u_l$  denotes the capacity of link  $l$ , and  $s_p$  represents a flow scaling parameter associated with discrete routing units. The first constraint enforces **flow conservation**, ensuring that the inflow equals the outflow at each intermediate node, and the second enforces **capacity constraints** limiting the flow on each link.

Traffic routing optimization is fundamental in modern operations research and telecommunications. It is widely applied in Internet traffic engineering, intelligent transportation systems, and large-scale communication networks, where

maintaining QoS guarantees (e.g., latency bounds or bandwidth reservations) is critical. An illustrative network example is shown in Figure 3.

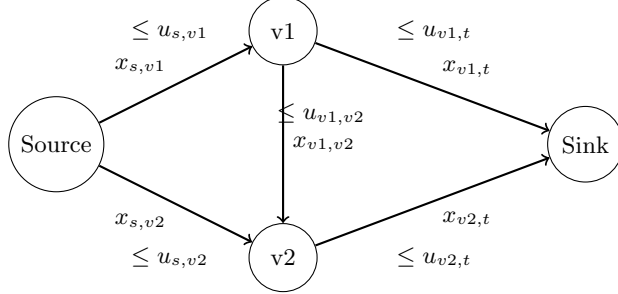


Figure 3: Traffic routing optimization: flows  $x_l$  travel from the source to the sink through intermediate nodes  $v_1$  and  $v_2$ . Flow conservation ensures that inflow equals outflow at each intermediate node, while link capacities  $u_l$  limit total traffic. The objective minimizes overall latency  $\sum_{l \in L} c_l(x_l)$  under QoS constraints.

**Wireless Network Spectrum Allocation (WNSA).** The WNSA problem [58] aims to assign available frequency bands to transmitters in a wireless network in order to minimize overall interference while satisfying channel availability and interference threshold constraints.

Let  $T$  denote the set of wireless transmitters (e.g., base stations, access points, or other transmitting devices) and  $F$  denote the set of available frequency bands (channels). Each transmitter  $i \in T$  must be assigned exactly one frequency  $f \in F$ . When two transmitters  $i, j \in T$  are assigned frequencies that cause overlapping signals or nearby spectral leakage, they generate interference quantified by a nonlinear function  $I_{ij}(x_i, x_j)$ . The objective is to minimize the total interference across all transmitter pairs while maintaining acceptable signal quality:

$$\min_x \sum_{i,j \in T} I_{ij}(x_i, x_j).$$

The WNSA problem can be formulated as the following mixed-integer nonlinear program:

$$\begin{aligned} \min & \sum_{i,j \in T} I_{ij}(x_i, x_j) \\ \text{s.t. } & \sum_{f \in F} x_{if} = 1, \quad \forall i \in T, \\ & I_{ij}(x_i, x_j) \leq \delta, \quad \forall i, j \in T, \\ & x_{if} \in \{0, 1\}, \quad \forall i \in T, f \in F, \end{aligned} \tag{12}$$

where  $x_{if} = 1$  if transmitter  $i$  is assigned frequency  $f$ , and 0 otherwise;  $I_{ij}(x_i, x_j)$  is a nonlinear interference function measuring signal overlap or channel conflict between transmitters  $i$  and  $j$ ;  $\delta > 0$  is the allowable interference threshold, generally  $\delta \in (0, \infty)$ . The first constraint ensures that each transmitter is assigned exactly one frequency band, while the second restricts the interference between any two transmitters to remain below the threshold  $\delta$ .

If channel interference is symmetric, then  $I_{ij}(x_i, x_j) = I_{ji}(x_j, x_i)$ . The parameter  $\delta > 0$  denotes the permissible interference threshold, typically determined by system QoS limits.

The WNSA problem is fundamental in wireless communications and network optimization. Applications include dynamic spectrum management in cognitive radio networks, frequency assignment in cellular and Wi-Fi systems, and interference-aware resource scheduling in 5G and next-generation wireless infrastructures. An illustrative example is shown in Figure 4.

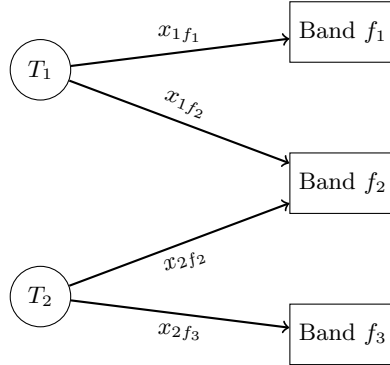


Figure 4: Wireless spectrum allocation: transmitters  $T_1$  and  $T_2$  must each be assigned one frequency band  $f \in F$ . Assignment variables  $x_{if}$  indicate chosen bands, while interference constraints  $I_{ij}(x_i, x_j) \leq \delta$  limit simultaneous use of conflicting channels.

**Energy-Efficient Network Design (EEND).** The EEND problem aims to design a communication or data network that minimizes total energy consumption by activating only a subset of available links and devices, while maintaining network connectivity and satisfying all traffic demands.

Let  $G = (V, L)$  be a directed or undirected graph where  $V$  denotes the set of network nodes and  $L$  the set of candidate links. Each link  $l \in L$  incurs an energy cost represented by a nonlinear function  $E_l(x_l)$ , where  $x_l \in \{0, 1\}$  is a binary variable indicating whether the link  $l$  is active ( $x_l = 1$ ) or inactive ( $x_l = 0$ ). The total energy consumption must not exceed the upper limit  $\bar{e}$ , which represents the available network energy budget ensuring feasibility. Let  $\delta(v)$  denote the

set of links incident to node  $v$ , and let  $K$  denote the set of traffic demands, where each  $d_k$  specifies the required flow or capacity to be supported in the network. The objective is to select a subset of links that minimizes total energy consumption while ensuring full connectivity and demand satisfaction.

The EEND problem can be formulated as the following mixed-integer nonlinear program:

$$\begin{aligned} \min \quad & \sum_{l \in L} E_l(x_l) \\ \text{s.t.} \quad & \sum_{l \in \delta(v)} x_l \geq 1, \quad \forall v \in V, \\ & \sum_{l \in \delta(v)} x_l \geq d_k, \quad \forall k \in K, \\ & \sum_{l \in L} E_l(x_l) \leq \bar{e}, \\ & x_l \in \{0, 1\}, \quad \forall l \in L. \end{aligned} \tag{13}$$

The first constraint ensures that each node in the network has at least one active link, thereby maintaining overall connectivity. The second constraint guarantees that the network can accommodate all required traffic demands  $d_k$ . The third constraint limits the total energy consumption to the predefined energy budget  $\bar{e}$  (which represents the total available energy budget limiting network operation costs). The binary decision variables  $x_l$  activate or deactivate network links, enabling an energy-efficient configuration that balances operational cost and performance.

The EEND problem is a critical problem in sustainable telecommunications and computing infrastructures. It arises in green data center management, smart grid communication systems, and next-generation Internet backbones, where energy savings must be achieved without compromising connectivity or service quality. An illustrative example is presented in Figure 5.

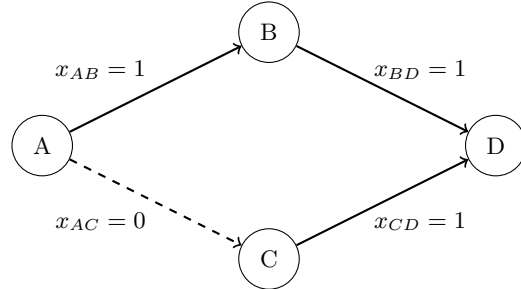


Figure 5: Energy-efficient network design: nodes A–D are connected by links. Binary variables  $x_l$  indicate whether a link is active (solid) or inactive (dashed). The objective is to minimize  $\sum_l E_l(x_l)$  subject to connectivity and demand constraints.

**Load Balancing in Data Centers (LBDC).** The LBDC problem [1] seeks to distribute workloads across multiple servers in a way that minimizes total energy consumption while ensuring that capacity and latency constraints are satisfied.

Consider a data center system consisting of a set of servers (or computing nodes)  $J$  and a set of workloads or tasks  $\mathcal{S}$  to be processed. Each workload  $j \in J$  must be allocated among servers according to the system demand  $d_j$ . Each server  $i \in \mathcal{S}$  has a finite processing capacity  $u_i$  and incurs a power consumption  $P_i(x_i)$ , which is typically a nonlinear increasing function of its utilization  $x_i$ . The objective is to determine an allocation of workloads that minimizes the total energy consumed while ensuring demand satisfaction and respecting server capacities.

The LBDC problem can be formulated as the following nonlinear mixed-integer program:

$$\begin{aligned} \min \quad & \sum_{i \in \mathcal{S}} P_i(x_i) \\ \text{s.t.} \quad & \sum_{i \in \mathcal{S}} x_{ij} = d_j, \quad \forall j \in J, \\ & \sum_{j \in J} x_{ij} \leq u_i, \quad \forall i \in \mathcal{S}, \\ & x_i \in s_i \mathbb{Z}_+, \quad \forall i \in \mathcal{S}, \end{aligned} \tag{14}$$

where  $x_{ij}$  denotes the allocation of workload  $j$  to server  $i$ , and  $x_i$  represents the total workload handled by server  $i$ . The first constraint ensures that each workload demand  $d_j$  is completely satisfied by the aggregate allocation from all servers. The second constraint enforces server capacity limits, guaranteeing that no server operates beyond its capacity  $u_i$ . The final constraint defines the discrete or quantized nature of the workload units, where  $s_i$  denotes a scaling factor corresponding to the granularity of tasks processed by server  $i$ .

The LBDC problem is central to modern cloud computing and distributed computing infrastructures. It underpins energy-aware scheduling, dynamic server provisioning, and adaptive workload management in large-scale data centers. Optimally balancing load across servers reduces both energy costs and operational latency while improving system reliability and sustainability. Empirical studies such as [7] demonstrate the practical impact of energy-aware load balancing in large-scale cloud data centers. By dynamically consolidating workloads and adapting server utilization through heuristic or migration-based strategies, significant reductions in power consumption can be achieved while maintaining quality-of-service guarantees. This aligns closely with the optimization framework in (14), which formalizes workload distribution and capacity constraints as an energy-minimization problem under discrete operational limits. An illustrative example is shown in Figure 6.

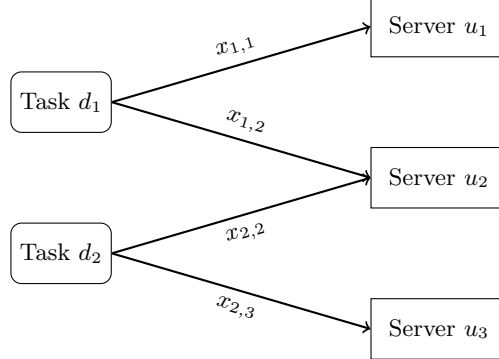


Figure 6: Load balancing in data centers: workloads  $d_j$  are distributed among servers with capacity  $u_i$ . Variables  $x_{ij}$  denote the amount of workload assigned from task  $j$  to server  $i$ . The objective minimizes total power consumption  $\sum_i P_i(x_i)$  subject to demand and capacity constraints.

**Network Security and Intrusion Detection (NSID).** The NSID problem [42] seeks to determine the optimal placement of security devices—such as firewalls, intrusion detection systems (IDS), or monitoring sensors—to minimize total deployment cost while ensuring complete coverage of critical network nodes and links.

Let  $G = (V, E)$  represent a communication network, where  $V$  is the set of nodes (e.g., routers, switches, or servers) that must be protected and  $E$  is the set of links connecting them. Let  $N$  denote the set of candidate locations where sensors or IDS devices can be deployed. Each device  $i \in N$  incurs a deployment cost  $c_i$  and provides coverage to a subset of nodes incident to it, denoted by  $\delta(v)$ . The binary decision variable  $x_i$  indicates whether a device is deployed at location  $i$  ( $x_i = 1$ ) or not ( $x_i = 0$ ). The objective is to minimize the total installation cost while maintaining full network coverage and adhering to a deployment budget  $\gamma$ .

The NSID problem can be formulated as the following binary integer program:

$$\begin{aligned}
\min \quad & \sum_{i \in N} c_i x_i \\
\text{s.t.} \quad & \sum_{j \in \delta(v)} x_j \geq 1, \quad \forall v \in V, \\
& \sum_{i \in N} c_i x_i \leq \gamma, \\
& x_i \in \{0, 1\}, \quad \forall i \in N.
\end{aligned} \tag{15}$$

Here, the parameter  $\gamma > 0$  denotes the total cost budget for deploying security devices.

The first constraint ensures that every network node  $v \in V$  is covered by at least one active security device—this is the **coverage constraint**. The second constraint imposes a total cost limit  $\gamma$ , which represents the available deployment budget or a general resource limitation such as power, storage, or bandwidth. The binary variables  $x_i$  determine the selection and placement of devices across the network.

This formulation captures a broad class of problems in cybersecurity and network defense, including optimal placement of firewalls, intrusion detection systems, and monitoring agents. It applies to enterprise networks, cloud infrastructures, and Internet of Things (IoT) environments where resources for protection are limited and efficient coverage is critical. An illustrative example is shown in Figure 7.

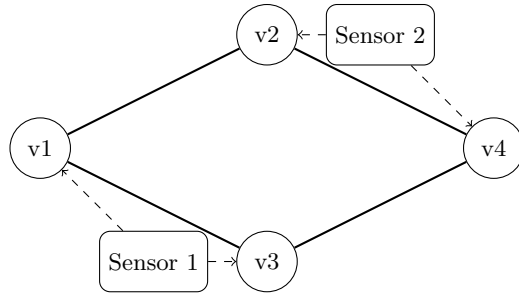


Figure 7: Network security and intrusion detection: binary decision variables  $x_i$  determine whether sensors are deployed. Sensor 1 covers nodes  $v_1$  and  $v_3$ , while Sensor 2 covers nodes  $v_2$  and  $v_4$ . The objective minimizes total cost subject to coverage and budget constraints.

**Transport Route Selection (TRS).** This subsection discusses the TRS problem as a representative example of optimization models that incorporate **logical (disjunctive) constraints**. Two complementary formulations are presented to highlight both the *practical* and *theoretical* aspects of such problems. The first example provides a **complete mixed-integer linear programming (MILP)** model capturing transportation costs, flow conservation, capacity limits, and logical route-selection rules within a realistic network. The second, titled *Disjunctive Representation of Alternative Routes*, abstracts the same idea into a **compact logical form** that isolates the essential disjunction between alternative feasible routes. Together, these examples illustrate how disjunctive conditions arise naturally in transport planning and how they can be modeled either as part of an integrated MILP system or as a standalone logical construct—bridging the gap between **network optimization practice** and the **foundations of DisP**.

**Example 1: Transport Route Selection.** The TRS problem [22] seeks to determine an optimal set of transportation routes that minimize total shipping cost while satisfying logical, capacity, and supply–demand balance constraints. This problem frequently arises in logistics network design, multimodal transportation planning, and supply chain optimization.

Let  $\mathcal{S}$  denote the set of supply nodes,  $D$  the set of demand nodes, and  $R$  the set of feasible transportation routes. For each route  $(i, j)$ , the decision variable  $x_{ij}$  represents the quantity of goods transported, and the binary variable  $y_{ij}$  indicates whether route  $(i, j)$  is selected ( $y_{ij} = 1$ ) or not ( $y_{ij} = 0$ ). The unit transportation cost on route  $(i, j)$  is denoted by  $c_{ij}$ , and  $u_{ij}$  denotes its capacity limit. Each node  $i$  is associated with a supply or demand quantity  $b_i$ , where  $b_i > 0$  for suppliers and  $b_i < 0$  for consumers. The objective is to minimize the total transportation cost while maintaining network feasibility and logical route consistency.

The TRS problem can be formulated as the following mixed-integer linear program:

$$\begin{aligned} \min \quad & \sum_{(i,j)} c_{ij} x_{ij} \\ \text{s.t.} \quad & \sum_j x_{ij} - \sum_j x_{ji} = b_i, \quad \forall i \in \mathcal{S} \cup D, \\ & \sum_{(i,j) \in R} y_{ij} \geq 1, \\ & y_{ij} + y_{ik} \leq 1, \quad \forall i, j, k, \\ & y_{ij} \leq y_{kl}, \\ & x_{ij} \leq u_{ij} y_{ij}, \quad \forall (i, j), \\ & y_{ij} \in \{0, 1\}, \quad \forall (i, j), \\ & x_{ij} \geq 0, \quad \forall (i, j). \end{aligned} \tag{16}$$

In this formulation, the first constraint enforces **flow conservation**, ensuring that the net flow at each node equals its supply or demand  $b_i$ . The second to fourth constraints constitute the **disjunctive constraints**, which ensure logical route selection rules. Specifically, the second constraint guarantees that at least one feasible route is chosen, the third prevents conflicting or parallel routes from being activated simultaneously, and the fourth enforces hierarchical or dependency relationships between routes. The fifth constraint imposes **capacity limits** on each selected route. The binary variables  $y_{ij}$  determine which routes are active, while continuous variables  $x_{ij}$  capture the flow of goods along those routes.

Transport route selection models are used in multimodal logistics systems, freight network optimization, and supply chain planning. They help determine the most cost-effective configuration of shipping lanes, trucking paths, or rail

connections while respecting infrastructure capacity and demand fulfillment. An illustrative example is shown in Figure 8.

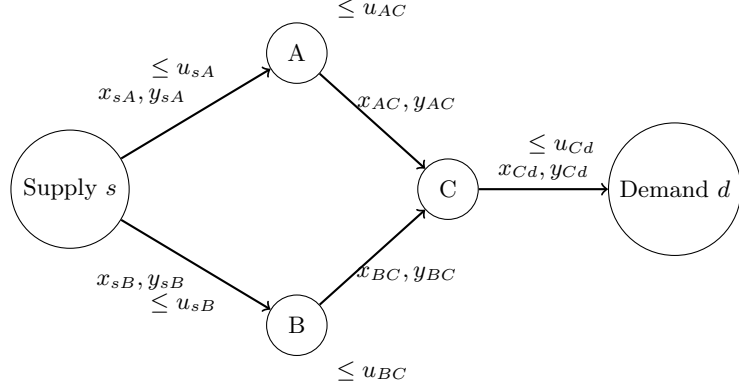


Figure 8: Transport route selection: goods flow from a supply node  $s$  to a demand node  $d$  through alternative routes (via  $A$  or  $B$  to  $C$ ). Decision variables  $x_{ij}$  represent transported quantities, while binary variables  $y_{ij}$  indicate selected routes. Capacity constraints  $u_{ij}$  restrict feasible flows, and disjunctive constraints prevent conflicting or redundant route choices.

**Example 2: Disjunctive Representation of Alternative Routes.** Consider a transportation network where goods can be shipped through one of several alternative routes. Suppose that if route A is chosen, the flow variables  $x$  must satisfy capacity and travel-time constraints  $h^1(x) \leq 0$ , whereas if route B is chosen, the constraints  $h^2(x) \leq 0$  apply. This naturally leads to a disjunctive formulation

$$(h^1(x) \leq 0) \vee (h^2(x) \leq 0),$$

which captures the logical choice between route A and route B. Such modeling is typical in logistics and supply chain optimization, where route alternatives, congestion thresholds, or contractual restrictions require disjunctive conditions; for example, see Figure 9.

**Machine Configuration in Manufacturing (MCM).** We here discuss the MCM problem as a canonical example of **disjunctive modeling** in production and scheduling systems. Two complementary formulations are presented to highlight both the *practical* and *theoretical* aspects of disjunctions in manufacturing optimization. The first example introduces a MINLP formulation that integrates task assignment, capacity, precedence, and sequencing constraints within a flexible manufacturing environment. The second, titled *Disjunctive Representation of Machine Alternatives*, abstracts these ideas into a **logical**

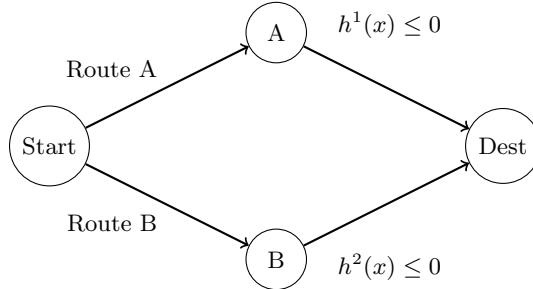


Figure 9: Transport route selection: goods can be sent either via Route A or Route B. Each route is associated with its own capacity and travel-time constraints ( $h^1(x) \leq 0$  or  $h^2(x) \leq 0$ ). The disjunction enforces that at least one feasible route must be chosen.

**either-or structure** that isolates the essential technological disjunction between alternative machine configurations. Together, these examples show how production scheduling can be formulated either as an integrated MILP/MINLP model or as a logical disjunction of machine-specific subsystems, linking practical industrial scheduling problems with the **DisP** framework introduced by Balas [4].

**Example 1: Machine Configuration in Manufacturing.** The MCM problem [4] aims to determine the optimal assignment of tasks to machines and their execution sequence in order to minimize total operational cost while satisfying capacity, precedence, and scheduling constraints.

Let  $T$  denote the set of manufacturing tasks and  $M$  the set of available machines. Each task  $i \in T$  must be processed by exactly one machine  $j \in M$ . The binary variable  $x_{ij}$  equals 1 if task  $i$  is assigned to machine  $j$  and 0 otherwise. The start and completion times of task  $i$  are represented by  $s_i$  and  $C_i$ , respectively. Each task  $i$  has a known processing time  $p_i$ , and assigning it to machine  $j$  incurs a cost  $d_{ij}$ . The scheduling of tasks on a shared machine is controlled by precedence and non-overlapping constraints, where  $h$  is a sufficiently large positive constant (big- $M$ ) used to linearize disjunctive relations. The objective is to minimize the total cost of task-machine assignments while ensuring that each task is processed exactly once, machine capacities are respected, and precedence constraints are maintained.

The MCM problem can be formulated as the following mixed-integer nonlinear

program:

$$\begin{aligned}
\min \quad & \sum_{i \in T} \sum_{j \in M} d_{ij} x_{ij} \\
\text{s.t.} \quad & \sum_{j \in M} x_{ij} = 1, \quad \forall i \in T, \\
& s_i + p_i \leq s_k + h(1 - x_{ij}x_{kj}), \quad \forall i, k \in T, i \neq k, j \in M, \\
& C_i \leq s_k, \quad \forall i, k \in T, \\
& C_i = s_i + p_i, \quad \forall i \in T, \\
& x_{ij} \in \{0, 1\}, \quad \forall i \in T, j \in M, \\
& s_i \geq 0, \quad \forall i \in T, \\
& \text{either } s_i + p_i \leq s_k \text{ or } s_k + p_k \leq s_i, \quad \forall i, k \in T, i \neq k, j \in M.
\end{aligned} \tag{17}$$

The first constraint ensures that each task is assigned to exactly one machine (**task assignment constraint**). The second constraint prevents overlapping tasks on the same machine (**machine capacity constraint**) through a big- $M$  formulation. The third and fourth constraints define **precedence** and **completion time relations**. The fifth and sixth constraints specify binary and nonnegativity conditions, while the final disjunctive constraint enforces non-overlapping schedules for any pair of tasks assigned to the same machine. Here,  $h > 0$  is a sufficiently large constant (Big- $M$ ) satisfying  $h \gg \max_i p_i$ , ensuring that disjunctive scheduling constraints are correctly linearized.

Machine configuration models are fundamental to production planning and manufacturing systems. They are widely applied in job-shop scheduling, flexible manufacturing systems, and robotic cell operations, where efficient task assignment and sequencing directly influence throughput and energy consumption. An illustrative example is presented in Figure 10.

**Example 2: Disjunctive Representation of Machine Alternatives.** In a flexible manufacturing system, a product may be processed on one of several machines, each with its own setup cost and operating constraints. For instance, if the product is assigned to machine 1, then equality constraints  $g^1(x) = 0$  and inequalities  $h^1(x) \leq 0$  enforce the technical requirements of machine 1. If instead machine 2 is chosen, the feasible set is defined by a different system  $g^2(x) = 0$ ,  $h^2(x) \leq 0$ . The assignment can be written disjunctively as

$$(g^1(x) = 0, h^1(x) \leq 0) \vee (g^2(x) = 0, h^2(x) \leq 0).$$

This illustrates how disjunctions capture *either-or* technological choices. In practice, the inclusion of integer variables ensures that only one configuration

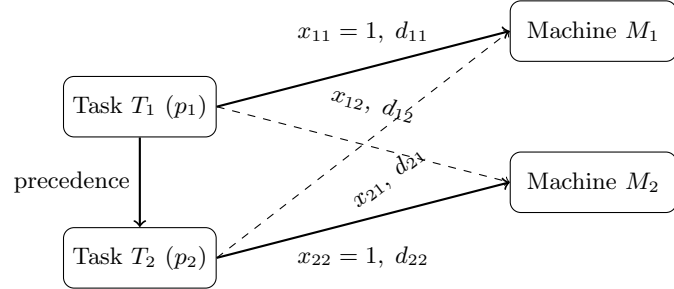


Figure 10: Machine configuration in manufacturing: each task  $i$  must be assigned to exactly one machine  $j$ , with binary variable  $x_{ij}$ . Costs  $d_{ij}$  depend on the assignment. Here, Task  $T_1$  is assigned to Machine  $M_1$  and Task  $T_2$  to Machine  $M_2$ . Dashed arrows represent alternative assignments. A precedence constraint requires  $T_1$  to finish before  $T_2$  starts.

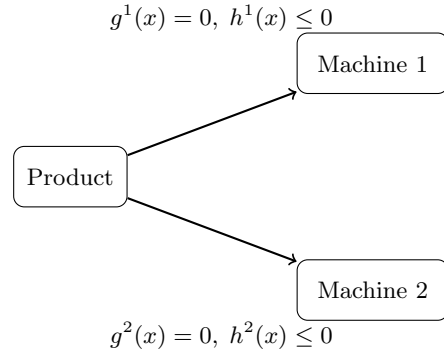


Figure 11: Machine configuration: a product can be assigned either to Machine 1 or Machine 2. Each machine has its own equality and inequality constraints defining feasibility. The disjunctive formulation ensures that exactly one machine configuration is selected.

is activated, which is critical in mixed-integer **DisP** (MIDNP); for example, see Figure 11.

The optimization models and graph-based formulations above provide the foundation for integrating data–driven and learning–based heuristics. In the following section, we introduce the ML and RL frameworks that will later enhance these classical solvers.

## 7 GNNs for Graph Optimization

Graph optimization provides a natural interface between combinatorial optimization and modern learning-based reasoning. Many canonical CSP and SAT formulations—such as shortest path, spanning tree, max flow, and graph coloring—can be represented as optimization problems on graphs. This section first revisits these classical graph formulations to illustrate the geometric and algebraic structure underlying combinatorial reasoning, and then demonstrates how GNNs extend these ideas into a differentiable, learning-based framework.

This section examines how ideas from classical graph optimization connect with modern GNN architectures. Message-passing networks mirror the core operations of many graph algorithms, such as propagation, aggregation, and local constraint evaluation, while allowing these operations to be learned from data. This makes GNNs a natural fit for problems where reasoning depends on relational structure. At the same time, their ability to encode structural constraints within learned representations provides a practical basis for hybrid symbolic and statistical methods, enabling scalable and adaptive solutions to graph-based decision problems.

The formal definitions and mathematical formulations of the classical graph optimization problems—such as the shortest path, minimum spanning tree, maximum flow, minimum cut, graph coloring, and traveling salesman—are provided in Section 7.2, where each is expressed as a linear or mixed-integer program forming the foundation of the GNN learning framework developed here. Figure 12 summarizes these core problems and their relationships, illustrating how diverse combinatorial tasks can be unified under a common graph–optimization structure widely studied in operations research [28].

### 7.1 Overview of Graph Optimization Problems

Beyond integer formulations, another common representation for combinatorial optimization problems is the **graph**. A graph  $G$  is defined as a pair  $(V, E)$ , where  $V = \{v_1, v_2, \dots, v_n\}$  is the set of vertices (or nodes) and  $E = \{(v_i, v_j) \mid v_i, v_j \in V, v_i \neq v_j\}$  is the set of edges. Each edge  $(v_i, v_j) \in E$  may indicate

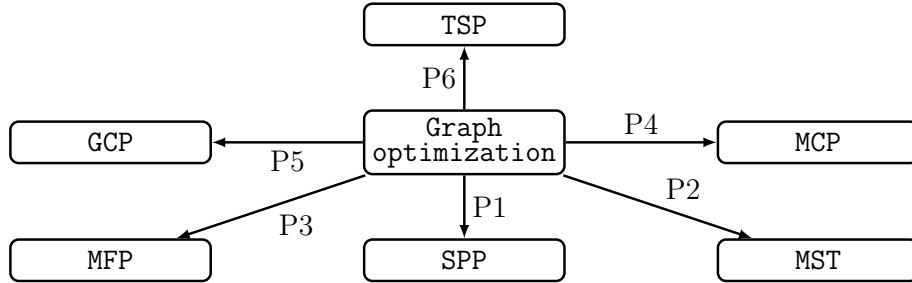


Figure 12: Flowchart for core graph optimization problems (P1–P6). SPP—shortest path, MST—minimum spanning tree, MFP— maximum flow, MCP—minimum cut, GCP—graph coloring, and TSP—traveling salesman. These canonical problems serve as the analytical foundation for GNN-based optimization models.

the presence of a connection ( $e_{ij} \in \{0, 1\}$ ), a numerical weight ( $e_{ij} \in \mathbb{R}$ ), or an attribute such as a color ( $e_{ij} \in \mathbf{c} = \{\text{blue}, \text{red}\}$ ). See [12] for a comprehensive monograph on graph theory.

Graphs can be undirected or directed. In an undirected graph,  $e_{ij} = 1$  implies  $e_{ji} = 1$ . Undirected graphs typically represent symmetric relationships, while directed graphs (or “digraphs”) represent asymmetric interactions—such as influence in a statistical model or the flow of a commodity in a network. Cyclicality is an important concern in digraphs, and a Directed Acyclic Graph (DAG), wherein there are no cycles, is often sought to define the structure of influence in a model, wherein a cycle can indicate the model being vacuous. See [5] for a comprehensive text on digraphs. A recent deep line of work explores the cohomology of digraphs; see [20, 30].

Combinatorial optimization problems on graphs can typically be redefined in terms of some mixed-integer problem, indeed with  $e_{ij}$  treated as a binary or real-valued decision variable. However, while such a translation can enable the use of generic integer programming software to solve such problems, one should be careful before resorting to this “brute force” type of approach. The structure of graphs yields insight into considerably faster algorithms that use graph properties, which include a host of higher-order geometry, e.g., cliques, that can be informative in the design and structure of algorithms. See the text [28] for further details on combinatorial optimization.

## 7.2 Classical Graph Optimization Problems

**Shortest Path Problem (SPP).** The SPP aims to determine the path of minimum total weight between two specified vertices in a weighted graph.

Let  $G = (V, E)$  be a directed (or undirected) graph with nonnegative edge weights (or costs)  $c_{ij} \geq 0$  for all  $(i, j) \in E$ . Two distinct vertices  $s, t \in V$  are designated as the *source* and *destination* (or *target*) nodes, respectively. The objective is to find a path from  $s$  to  $t$  that minimizes the total cost:

$$\min_{P \in \mathcal{P}_{s,t}} c(P) = \sum_{(i,j) \in P} c_{ij},$$

where  $\mathcal{P}_{s,t}$  denotes the set of all  $s$ - $t$  paths in  $G$ .

The SPP can equivalently be formulated as a flow-based linear program:

$$\begin{aligned} & \min \quad \sum_{(i,j) \in E} c_{ij} x_{ij} \\ \text{s.t.} \quad & \sum_{\{j | (i,j) \in E\}} x_{ij} - \sum_{\{j | (j,i) \in E\}} x_{ji} = \begin{cases} 1, & \text{if } i = s, \\ -1, & \text{if } i = t, \\ 0, & \text{otherwise,} \end{cases} \\ & x_{ij} \geq 0, \quad \forall (i, j) \in E, \end{aligned} \tag{18}$$

where the decision variable  $x_{ij}$  represents the amount of flow on edge  $(i, j)$ . In an integer setting,  $x_{ij} = 1$  if edge  $(i, j)$  lies on the shortest  $s$ - $t$  path, and  $x_{ij} = 0$  otherwise. The first set of constraints enforces *flow conservation*: one unit of flow is sent from the source  $s$  and received at the sink  $t$ , ensuring a continuous path from  $s$  to  $t$ .

The shortest path problem is fundamental in operations research, with applications in transportation and logistics, telecommunication and network routing, and project scheduling and management. An illustrative example is provided in Figure 13.

**Minimum Spanning Tree (MST).** The MST problem seeks a subset of edges that connects all vertices in a connected, weighted graph with the minimum possible total edge cost.

Let  $G = (V, E)$  be an undirected and connected graph, where  $V$  is the set of vertices and  $E$  is the set of edges. Each edge  $(i, j) \in E$  is associated with a nonnegative weight (or cost)  $c_{ij} \geq 0$ . A *spanning tree* of  $G$  is a subgraph  $T = (V, E_T)$  that connects all vertices of  $V$  without forming any cycles. The objective of the MST problem is to find such a spanning tree  $T$  that minimizes

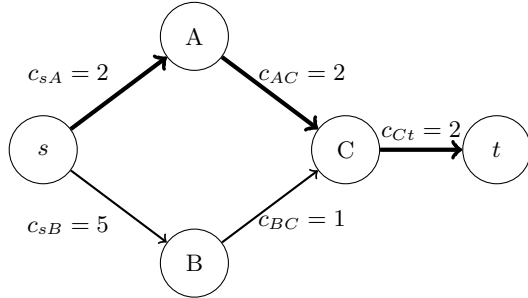


Figure 13: Shortest path problem (SPP): given edge weights  $c_{ij}$ , the goal is to find a path from  $s$  to  $t$  with minimum total cost. Here, the optimal path (thick) is  $s \rightarrow A \rightarrow C \rightarrow t$  with cost  $2 + 2 + 2 = 6$ .

the total edge cost:

$$\min_{E_T \subseteq E} c(E_T) = \sum_{(i,j) \in E_T} c_{ij}.$$

The MST problem can be expressed as the following integer program:

$$\begin{aligned} \min & \quad \sum_{(i,j) \in E} c_{ij} x_{ij} \\ \text{s.t.} & \quad \sum_{(i,j) \in E} x_{ij} = |V| - 1, \\ & \quad \sum_{(i,j) \in E(S)} x_{ij} \leq |S| - 1, \quad \forall S \subset V, S \neq \emptyset, \\ & \quad x_{ij} \in \{0, 1\}, \quad \forall (i, j) \in E, \end{aligned} \tag{19}$$

where  $x_{ij} = 1$  if edge  $(i, j)$  is included in the spanning tree and  $x_{ij} = 0$  otherwise. The first constraint ensures the correct number of edges in a spanning tree, and the second (subtour elimination) prevents cycles.

The MST problem has numerous applications in operations research and computer science, including cluster analysis in data science, supply chain and transportation network design, and infrastructure planning. An illustrative example is shown in Figure 14.

**Maximum Flow Problem (MFP).** The MFP seeks to determine the greatest possible amount of flow that can be sent from a designated source vertex to a designated sink vertex through a capacitated network.

Let  $G = (V, E)$  be a directed graph where each edge  $(i, j) \in E$  has a nonnegative capacity  $u_{ij} \geq 0$  representing the maximum permissible flow along that edge. Two distinct vertices  $s, t \in V$  are designated as the *source* and *sink* (or *target*) nodes, respectively. A *feasible flow* is a function  $f : E \rightarrow \mathbb{R}_+$  satisfying the

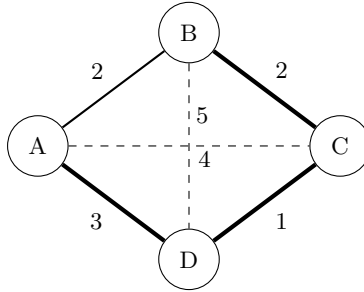


Figure 14: Minimum spanning tree (MST): the selected edges (thick) connect all vertices with minimum total weight  $3 + 2 + 1 = 6$ .

following:

1. **Capacity constraints:**  $0 \leq f_{ij} \leq u_{ij}$  for all  $(i, j) \in E$ ;
2. **Flow conservation:** for every vertex  $i \in V \setminus \{s, t\}$ ,

$$\sum_{j:(i,j) \in E} f_{ij} - \sum_{j:(j,i) \in E} f_{ji} = 0.$$

The goal is to maximize the total amount of flow leaving the source (equivalently, entering the sink):

$$\max_f \sum_{j:(s,j) \in E} f_{sj} - \sum_{j:(j,s) \in E} f_{js}.$$

The MFP can be formulated as the following linear program:

$$\begin{aligned} & \max_f \sum_{\{j|(s,j) \in E\}} f_{sj} - \sum_{\{j|(j,s) \in E\}} f_{js} \\ \text{s.t. } & \sum_{\{j|(i,j) \in E\}} f_{ij} - \sum_{\{j|(j,i) \in E\}} f_{ji} = 0, \quad \forall i \in V \setminus \{s, t\}, \\ & 0 \leq f_{ij} \leq u_{ij}, \quad \forall (i, j) \in E, \end{aligned} \tag{20}$$

where  $f_{ij}$  denotes the flow on edge  $(i, j)$  and  $u_{ij}$  its capacity. The objective maximizes the net outflow from the source, subject to flow conservation at all intermediate nodes and edge capacity constraints.

The MFP has broad applications in operations research and network optimization, including transportation and logistics planning, communication and data network design, and resource or workforce assignment. An illustrative example is provided in Figure 15.

**Minimum Cut Problem (MCP).** The MCP seeks to partition the vertices of a graph into two disjoint sets such that the total weight of the edges crossing the partition is minimized.

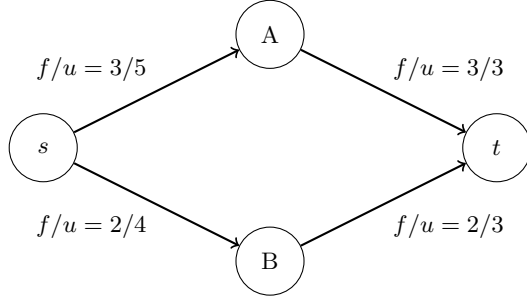


Figure 15: Maximum flow problem (MFP): flows  $f_{ij}$  (numerators) are assigned on each edge subject to capacity limits  $u_{ij}$  (denominators). The maximum flow from  $s$  to  $t$  in this example is 5.

Let  $G = (V, E)$  be a directed (or undirected) graph with nonnegative edge capacities (or costs)  $c_{ij} \geq 0$  for all  $(i, j) \in E$ . Two distinct vertices  $s, t \in V$  are designated as the *source* and *sink* (or target), respectively. The goal is to find a partition  $(S, T)$  of  $V$  satisfying  $s \in S$ ,  $t \in T$ , that minimizes the total capacity of edges from  $S$  to  $T$ :

$$\min_{(S,T)} c(S, T) = \sum_{(i,j) \in E, i \in S, j \in T} c_{ij}.$$

The minimum cut problem can be expressed equivalently as the following integer program:

$$\begin{aligned} \min & \quad \sum_{(i,j) \in E} c_{ij} x_{ij} \\ \text{s.t.} & \quad x_{ij} \geq y_i - y_j, \quad \forall (i, j) \in E, \\ & \quad y_s = 1, \quad y_t = 0, \\ & \quad 0 \leq x_{ij} \leq 1, \quad y_i \in \{0, 1\}, \quad \forall i \in V, (i, j) \in E, \end{aligned} \tag{21}$$

where  $y_i$  indicates the partition assignment of vertex  $i$  ( $y_i = 1$  if  $i \in S$ ,  $y_i = 0$  if  $i \in T$ ), and  $x_{ij}$  is an indicator variable equal to 1 if edge  $(i, j)$  crosses the cut from  $S$  to  $T$  and 0 otherwise.

The minimum cut problem arises in various domains of operations research, including network reliability analysis, supply chain optimization, and project scheduling and resource allocation. An illustrative example is provided in Figure 16.

**Graph Coloring Problem (GCP).** The GCP seeks to assign colors to vertices of a graph such that no two adjacent vertices share the same color, while minimizing the total number of colors used.

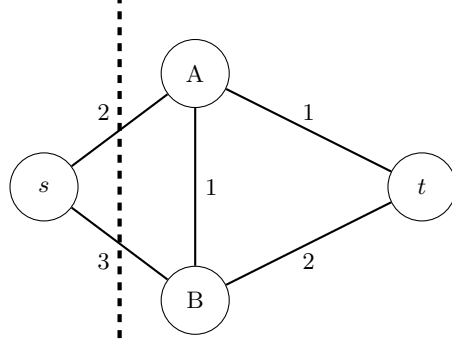


Figure 16: Minimum cut problem (MCP): the dashed line separates  $\{s\}$  from  $\{A, B, t\}$ , cutting edges  $(s, A)$  and  $(s, B)$  with total cost  $2 + 3 = 5$ .

Let  $G = (V, E)$  be an undirected graph, where  $V$  is the set of vertices and  $E$  is the set of edges. A *proper coloring* of  $G$  assigns a color  $v \in [k] = \{1, 2, \dots, k\}$  to each vertex  $i \in V$  such that adjacent vertices receive different colors. The objective is to determine the smallest integer  $k$  (the *chromatic number*) for which such a coloring exists:

$$\min_{x, k} k.$$

The GCP can be formulated as the following integer program:

$$\begin{aligned} & \min_k \\ \text{s.t. } & x_{iv} + x_{jv} \leq 1, \quad \forall (i, j) \in E, \forall v \in [k], \\ & \sum_{v=1}^k x_{iv} = 1, \quad \forall i \in V, \\ & x_{iv} \in \{0, 1\}, \quad \forall i \in V, \forall v \in [k], \end{aligned} \tag{22}$$

where the binary decision variable  $x_{iv}$  equals 1 if vertex  $i$  is assigned color  $v$ , and 0 otherwise. The first set of constraints enforces that adjacent vertices cannot share the same color, while the second ensures that each vertex receives exactly one color. Minimizing  $k$  yields the smallest number of colors needed to properly color the graph.

The graph coloring problem is a classical NP-hard problem with widespread applications in operations research and computer science. Notable applications include register allocation in compiler design, frequency assignment in telecommunications, and task or resource scheduling in manufacturing systems. An illustrative example is shown in Figure 17.

**Traveling Salesman Problem (TSP).** The TSP seeks the shortest possible route that visits each vertex exactly once and returns to the starting vertex.

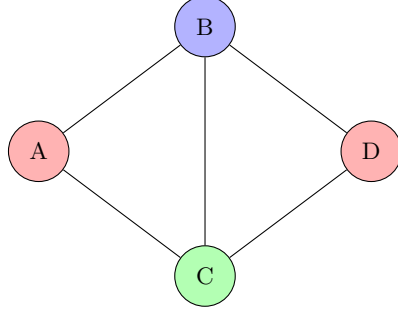


Figure 17: Graph coloring problem (GCP): each vertex is assigned a distinct color such that adjacent vertices differ. Here, three colors (red, blue, and green) suffice to color all vertices.

Let  $G = (V, E)$  be a complete directed (or undirected) graph where each edge  $(i, j) \in E$  is associated with a nonnegative travel cost (or distance)  $c_{ij} \geq 0$ . The objective is to determine a Hamiltonian cycle that visits every vertex in  $V$  exactly once and minimizes the total travel cost:

$$\min_x \sum_{(i,j) \in E} c_{ij} x_{ij}.$$

Here,  $x_{ij}$  is a binary decision variable equal to 1 if the salesman travels directly from city  $i$  to city  $j$ , and 0 otherwise.

The TSP can be expressed as the following integer linear program:

$$\begin{aligned} \min & \sum_{(i,j) \in E} c_{ij} x_{ij} \\ \text{s.t.} & \sum_{\{j | (i,j) \in E\}} x_{ij} = 1, \quad \forall i \in V, \\ & \sum_{\{i | (i,j) \in E\}} x_{ij} = 1, \quad \forall j \in V, \\ & \sum_{(i,j) \in E(S)} x_{ij} \leq |S| - 1, \quad \forall S \subset V, S \neq \emptyset, \\ & x_{ij} \in \{0, 1\}, \quad \forall (i, j) \in E, \end{aligned} \tag{23}$$

where the first two sets of constraints ensure that each city is visited exactly once and departed from exactly once, while the third set (subtour elimination constraints) prevents disconnected cycles (subtours).

The TSP is a cornerstone problem in combinatorial optimization and operations research, with broad applications in logistics and transportation, manufacturing and robotic routing, and scheduling and sequencing. An illustrative example is shown in Figure 18.

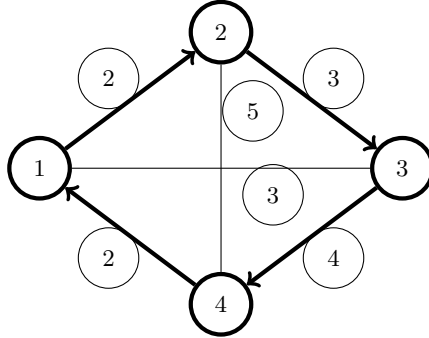


Figure 18: Traveling salesman problem (TSP): a tour visiting all vertices exactly once and returning to the start. The thick cycle represents the optimal route with minimum total cost.

The graph optimization problems discussed—shortest path, spanning tree, flow, cut, coloring, and TSP—form a hierarchy of classical combinatorial problems that underpin many OR applications. They also serve as natural domains for applying ML and RL techniques in subsequent sections.

### 7.3 GNN Architectures for Graph Problems

GNNs provide a unified framework to model and solve combinatorial optimization problems on graphs. Given a graph  $G = (V, E)$  with node features  $\{h_v^{(0)}\}_{v \in V}$  and edge features  $\{e_{uv}\}_{(u,v) \in E}$ , the GNN performs iterative *message passing* to update node and edge embeddings.

A general GNN layer follows the form:

$$h_v^{(k+1)} = \phi_{\text{upd}} \left( h_v^{(k)}, \sum_{u \in \mathcal{N}(v)} \phi_{\text{msg}}(h_u^{(k)}, e_{uv}) \right), \quad (24)$$

where  $\mathcal{N}(v)$  denotes the neighborhood of node  $v$ , and  $\phi_{\text{msg}}, \phi_{\text{upd}}$  are learnable functions implemented by multilayer perceptrons (MLPs). After  $K$  iterations, the final embeddings  $h_v^{(K)}$  capture multi-hop structural dependencies such as path lengths, connectivity, or capacities.

The learned embeddings are used by a decoder  $g_\theta$  to produce task-specific outputs:

$$\hat{y}_v = g_\theta(h_v^{(K)}), \quad \text{or} \quad \hat{y}_{uv} = g_\theta([h_u^{(K)}; h_v^{(K)}; e_{uv}]),$$

depending on whether the problem requires node-level or edge-level predictions. Here,  $[\cdot; \cdot]$  denotes vector concatenation.

**Variants.** Different GNN architectures specialize in distinct graph properties:

- **Graph Convolutional Networks (GCN)** [27]: use degree-normalized linear aggregation of neighboring node features.
- **Graph Attention Networks (GAT)** [54]: introduce learnable attention coefficients  $\alpha_{uv}$  to weight incoming messages adaptively.
- **Graph Isomorphism Networks (GIN)** [57]: maximize representational power by learning injective aggregation functions.
- **Message-Passing NNs (MPNN)** [19]: generalize the above by conditioning messages on edge attributes  $e_{uv}$  and allowing continuous feature updates.

**Training Objectives.** GNNs for combinatorial optimization are trained under either:

1. **Supervised learning:** minimizing  $\ell(\hat{y}, y^*)$  against ground-truth solutions (e.g., optimal paths or trees).
2. **Reinforcement learning:** maximizing the expected reward  $\mathbb{E}[R]$  through environment interactions, where  $R$  reflects the quality (e.g., inverse cost or feasibility) of the constructed solution.

The differentiable structure of Eq. (24) allows gradient-based learning of global combinatorial relationships without explicit enumeration.

**Complexity and Expressivity.** Theoretical results show that GNNs can emulate classical algorithms such as Bellman–Ford (for shortest paths) or Prim’s algorithm (for spanning trees) by embedding graph operations into differentiable message functions. Attention mechanisms enhance scalability by learning sparse dependencies across large graphs and selectively propagating information across critical edges.

## 7.4 Applications

The practical strength of GNNs emerges in their ability to approximate classical graph algorithms across a range of optimization tasks.

GNN-based solvers have been proposed for various graph optimization tasks, often trained on synthetic or real network instances where optimal or near-optimal solutions are known. The following subsections describe how GNN architectures approximate the core graph problems introduced earlier.

### 7.4.1 GNNs for SPP

In SPP, a GNN predicts edge-selection probabilities representing the likelihood of each edge belonging to the optimal path.

Let  $(s, t)$  denote the source and target nodes. Node embeddings  $h_v^{(K)}$  are processed by a decoder that estimates distance potentials:

$$\hat{d}_v = g_\theta(h_v^{(K)}), \quad \forall v \in V.$$

The predicted path  $\hat{P}_{s,t}$  is obtained by greedy edge selection following decreasing potential differences:

$$\hat{P}_{s,t} = \{(u, v) \in E : \hat{d}_u - \hat{d}_v \approx c_{uv}\},$$

where  $c_{uv}$  is the edge cost. Training minimizes the mean absolute error between predicted and true shortest distances  $d_v^*$  (computed by Dijkstra's algorithm):

$$L_{\text{SPP}} = \frac{1}{|V|} \sum_{v \in V} |\hat{d}_v - d_v^*|.$$

GNNs trained in this manner achieve near-optimal routing on unseen graphs and generalize across variable graph sizes.

### 7.4.2 GNNs for MST Learning

For the MST, each edge  $(i, j)$  is assigned a probability  $\hat{p}_{ij}$  of inclusion in the tree:

$$\hat{p}_{ij} = \sigma(g_\theta([h_i^{(K)}; h_j^{(K)}; e_{ij}])),$$

where  $\sigma(\cdot)$  denotes the sigmoid activation. The loss encourages the selection of low-cost edges that maintain connectivity while avoiding cycles:

$$L_{\text{MST}} = \sum_{(i,j) \in E} c_{ij} \hat{p}_{ij} + \lambda_1 \text{CyclePenalty}(\hat{p}) + \lambda_2 \text{DisconnectPenalty}(\hat{p}),$$

where  $\lambda_1, \lambda_2 > 0$  are penalty weights. Here,  $\text{CyclePenalty}(\hat{p})$  penalizes edge selections that create cycles, and  $\text{DisconnectPenalty}(\hat{p})$  penalizes disconnected components. This formulation mimics Kruskal's algorithm while providing a differentiable, end-to-end relaxable variant. Empirically, trained GNNs recover near-optimal trees and scale linearly with graph size.

### 7.4.3 GNNs for MFP/MCP Estimation

For MFP, edge embeddings encode both capacity  $u_{ij}$  and direction. A message-passing network predicts flow magnitudes  $\hat{f}_{ij}$  satisfying approximate conservation:

$$\hat{f}_{ij} = \text{ReLU}(g_\theta([h_i^{(K)}; h_j^{(K)}; u_{ij}])), \quad \sum_j (\hat{f}_{ij} - \hat{f}_{ji}) \approx 0, \quad \forall i \in V \setminus \{s, t\}.$$

The training objective minimizes violation of capacity and conservation while maximizing total feasible flow:

$$L_{\text{flow}} = \sum_{(i,j) \in E} [\max(0, \hat{f}_{ij} - u_{ij})]^2 + \sum_{i \neq s, t} \left( \sum_j (\hat{f}_{ij} - \hat{f}_{ji}) \right)^2 - \eta \sum_j \hat{f}_{sj},$$

where  $\eta > 0$  is a reward coefficient promoting larger feasible flows. MCP estimates can be derived from thresholded flow embeddings, consistent with the MFP/MCP duality.

### 7.4.4 GNNs for TSP Approximation

In the TSP, the model sequentially constructs a tour using an attention-based GNN (or Transformer) that selects the next node conditioned on the current partial route. Given node embeddings  $\{h_v^{(K)}\}$ , the policy network outputs selection probabilities:

$$\pi_\phi(v_t \mid s_t) = \text{softmax}(h_{v_t}^{(K)\top} W_\phi \bar{h}_t),$$

where  $\pi_\phi$  is the policy parameterized by  $\phi$ ,  $W_\phi$  is a learned projection matrix, and  $\bar{h}_t$  is the context vector summarizing the already visited nodes. The expected tour cost is minimized via

$$L_{\text{TSP}} = \mathbb{E}_{\pi_\phi} \left[ \sum_{(i,j) \in \text{tour}} c_{ij} \right],$$

where  $c_{ij}$  denotes the travel cost between cities  $i$  and  $j$ . Training employs reinforcement learning with reward  $R = -\text{tour length}$ , optimized via policy-gradient or PPO updates. This yields near-optimal tours competitive with classical heuristics (e.g., Lin–Kernighan) on moderate-size instances.

GNNs thus act as differentiable approximators of classical graph algorithms. Their message-passing architecture (Eq. (24)) captures structural information directly from graph topology, enabling amortized inference on unseen instances. When coupled with reinforcement objectives or hybrid CSP solvers, they provide a powerful, learning-based approach for large-scale combinatorial graph optimization.

## 8 Extended Examples and Algorithms in DisP

### 8.1 Background on Disjunctive Graphs and Logical Constraints

DisP provides a mathematical framework for representing scheduling and sequencing problems in which two operations competing for the same resource cannot overlap in time. Introduced by Balas [4], a *disjunctive graph*  $\mathcal{G} = (V, C \cup D)$  encodes a set of operations  $V$ , conjunctive arcs  $C$  representing precedence constraints, and disjunctive arcs  $D$  representing resource conflicts that must be ordered one way or the other.

**Classical Formulation.** Each operation  $i \in V$  has a start time  $x_i \in \mathbb{R}_+$  and processing duration  $p_i > 0$ . For any two operations  $(i, j)$  requiring the same machine, exactly one of the following disjunctions must hold:

$$x_i + p_i \leq x_j \quad \text{or} \quad x_j + p_j \leq x_i,$$

ensuring that no two jobs overlap on a shared resource. Precedence relations  $(i, j) \in C$  impose additional constraints  $x_i + p_i \leq x_j$ . The scheduling objective is often to minimize the *makespan*

$$C_{\max} = \max_{i \in V}(x_i + p_i),$$

subject to all conjunctive and disjunctive constraints.

This background establishes the classical and dynamic foundations of disjunctive scheduling on which subsequent sections build, including dynamic GNN–RL integration, risk-sensitive RL, and differentiable neural logic for disjunctive reasoning.

### 8.2 Learning-Enhanced DisP: Extended Case Studies

The following formulations and diagrams illustrate the mathematical structure and ML/RL integration for each domain in [24, Table 3].

**(1) Job–Shop Scheduling (GNN + RL on Disjunctive Graphs)** [38].  
The classical job–shop scheduling problem can be expressed as

$$\begin{aligned} \min_{x_i, C_{\max}} \quad & C_{\max} \\ \text{s.t.} \quad & x_i + p_i \leq x_j \vee x_j + p_j \leq x_i, \quad \forall (i, j) \in D, \\ & x_i + p_i \leq x_j, \quad \forall (i, j) \in C, \\ & C_{\max} \geq x_i + p_i, \quad \forall i \in V, \\ & x_i \geq 0, \end{aligned}$$

where  $x_i$  is the start time of operation  $i$ ,  $p_i$  its processing duration,  $C$  denotes precedence arcs, and  $D$  disjunctive (resource-conflict) arcs. A GNN encodes  $\mathcal{G} = (V, C \cup D)$  and an RL agent (e.g., PPO) learns a dispatching policy  $\pi_\phi(a_t | s_t)$  to minimize the makespan  $C_{\max}$ .

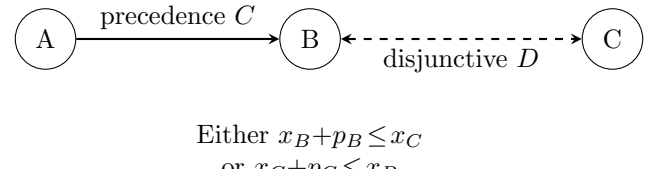


Figure 19: Disjunctive-graph representation of a job–shop scheduling instance.

**(2) Job–Shop Scheduling (Attention–based Deep RL)** [14]. The attention mechanism captures long-range dependencies among operations:

$$h_i = \text{attn}(Q, K, V)_i = \sum_{j \in V} \alpha_{ij} W_V x_j, \quad \alpha_{ij} = \frac{\exp((W_Q x_i)^\top (W_K x_j))}{\sum_k \exp((W_Q x_i)^\top (W_K x_k))}.$$

The RL policy  $\pi_\theta(a_t | s_t)$  selects the next operation based on attention-weighted embeddings, producing scalable, transferable schedules.

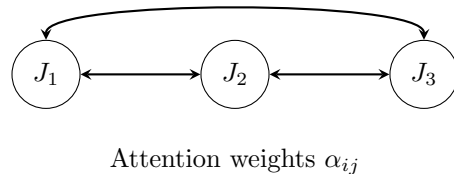


Figure 20: Attention-based encoding of global precedence and disjunction dependencies.

**(3) Chemical Production Scheduling (Distributional RL, CVaR)** [36].

Let  $Z^\pi(s, a)$  denote the random return distribution. A risk-sensitive scheduling problem minimizes expected downside loss:

$$\begin{aligned} \min_{\pi} \quad & \text{CVaR}_\alpha[-Z^\pi(s, a)] \\ \text{s.t.} \quad & x_i + p_i \leq x_j \vee x_j + p_j \leq x_i, \\ & h^l(x) \leq 0, g^l(x) = 0. \end{aligned}$$

The CVaR objective  $\text{CVaR}_\alpha(Z) = \mathbb{E}[Z | Z \leq F_Z^{-1}(\alpha)]$  penalizes the worst  $\alpha$ -fraction of outcomes, yielding safer policies for uncertain chemical-production systems.

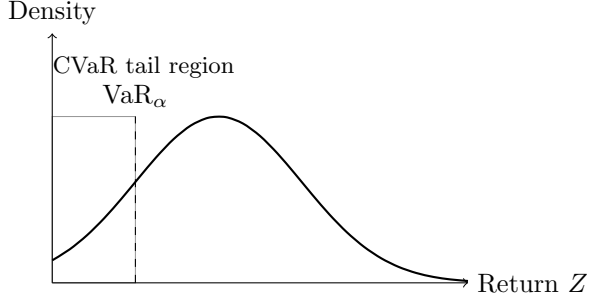


Figure 21: Illustration of the CVaR tail region for risk-sensitive RL scheduling.

**(4) Neuro-Symbolic RL (Inductive Logic Programming + RL)** [13].

Policies are expressed as differentiable logical combinations:

$$\pi(a|s) = \sigma \left( \sum_l w_l f_{\text{logic}}^l(s, a) \right), \quad f_{\text{disj}}(x) = 1 - \prod_i (1 - \sigma(w_i x_i)).$$

RL optimizes weights  $w_l$  to satisfy symbolic rules while preserving differentiability, yielding interpretable disjunctive decision structures.

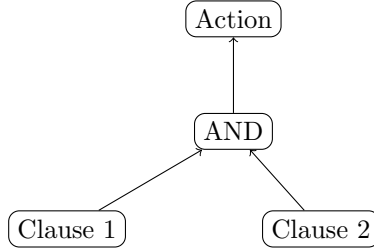


Figure 22: Differentiable logical composition in neuro-symbolic RL.

**(5) Program Analysis (Data–Driven Disjunctive Modeling) [23].** Program analysis with selective context sensitivity can be modeled by

$$\bigvee_{l=1}^L (g_l(x) = 0, h_l(x) \leq 0),$$

where each  $l$  denotes an execution context. ML models estimate probabilities  $p_l = \Pr(\text{select context } l | x)$  to guide which context or abstract domain to analyze.

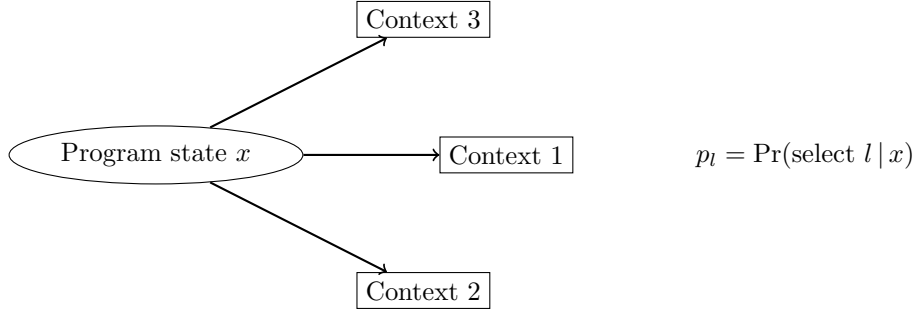


Figure 23: Disjunctive selection of analysis contexts guided by ML probabilities.

### 8.3 ML and RL Enhancements

Algorithm 17 demonstrates how differentiable neural logic integrates symbolic disjunctions into continuous neural optimization. In (S0<sub>17</sub>), the logical layer parameters  $w_i$ , temperature coefficient  $c$ , and predicate activations  $x_i \in [0, 1]$  are initialized to represent soft truth values. In (S1<sub>17</sub>), differentiable conjunction and disjunction functions  $f_{\text{conj}}(x)$  and  $f_{\text{disj}}(x)$  are computed using smooth sigmoid activations  $m_i = \sigma(cw_i)$ , providing continuous approximations of Boolean logic. During (S2<sub>17</sub>), the model evaluates a symbolic or RL-based loss  $L_{\text{logic}}$  and performs backpropagation through the logical operators to refine the weights  $w_i$ . Finally, (S3<sub>17</sub>) checks for convergence, halting when the loss or logical consistency stabilizes. Overall, Algorithm 17 enables NNs to reason over disjunctive relations in a differentiable manner, combining interpretability from logic with adaptability from learning.

Together, these learning-enhanced disjunctive frameworks demonstrate how neural architectures and RL can approximate, adapt, and optimize within complex disjunctive structures—bridging symbolic reasoning and data–driven decision-making.

---

**Algorithm 17** Differentiable neural logic learning for disjunctive reasoning

---

**Initialization**

(S0<sub>17</sub>) Initialize logic layer parameters  $w_i$ , temperature  $c > 0$ , and predicate activations  $x_i \in [0, 1]$ .

**repeat****Forward computation**

(S1<sub>17</sub>) Compute differentiable conjunction and disjunction  $f_{\text{conj}}(x)$  and  $f_{\text{disj}}(x)$  (defined by (9) in Section 2).

**Learning step**

(S2<sub>17</sub>) Evaluate symbolic or RL-based loss  $L_{\text{logic}}$ . Backpropagate through logical operators to update weights  $w_i$ .

**Convergence check**

(S3<sub>17</sub>) If loss  $L_{\text{logic}}$  stabilizes or logical accuracy converges, stop.

**until** convergence of differentiable logic representation

---

## 8.4 First-Order and Logical Constraint Satisfaction Problems (FOL-CSPs)

This subsection defines FOL-CSPs, which generalize classical SAT/CSP by allowing quantifiers and predicates over logical languages  $\mathcal{L} = (\mathcal{F}, \mathcal{P})$ , interpreted under models  $\mathcal{M}$ . It establishes quantified and relational reasoning beyond propositional logic. This concept is directly employed in Algorithm 18 (S0<sub>18</sub>–S3<sub>18</sub>) to construct and process neural-assisted FOL constraints and connects to Algorithm 9 (S1<sub>9</sub>) and Algorithm 10 (S1<sub>10</sub>) through grounding and propositional reduction.

While Boolean SAT solvers address propositional reasoning, many real-world domains require quantified and relational reasoning beyond propositional clauses. Typical examples include knowledge bases, planning with quantified preconditions, and constraint templates with parameters or relations between objects. These problems are naturally expressed as FOL-CSPs, which extend the classical triple  $(\mathcal{X}, \mathcal{D}, \mathcal{C})$  by defining constraints in a logical language  $\mathcal{L} = (\mathcal{F}, \mathcal{P})$  with function and predicate symbols.

A constraint  $c_j \in \mathcal{C}$  takes the general form

$$c_j(x_1, \dots, x_k) \equiv Q_1 y_1 \dots Q_r y_r \psi_j(x_1, \dots, x_k, y_1, \dots, y_r),$$

where each  $Q_i \in \{\forall, \exists\}$  is a quantifier and  $\psi_j$  is a quantifier-free conjunction or disjunction of atomic predicates over variables  $x_1, \dots, y_r$ . A **model**  $\mathcal{M} = (\mathcal{U}, I)$  provides a universe  $\mathcal{U}$  and an interpretation  $I$  assigning meaning to each

predicate and function symbol in  $\mathcal{L}$ . A solution is an assignment  $\mathcal{A} : \mathcal{X} \rightarrow \mathcal{U}$  such that  $\mathcal{M} \models c_j[\mathcal{A}]$  for all  $c_j \in \mathcal{C}$ .

**Definition 8.1** (FOL-CSP Instance). *A First-Order Constraint Satisfaction Problem is a tuple  $(\mathcal{L}, \mathcal{M}, \mathcal{X}, \mathcal{C})$ , where  $\mathcal{L}$  is a logical language,  $\mathcal{M}$  its interpretation structure,  $\mathcal{X}$  a finite set of logical variables, and  $\mathcal{C}$  a set of first-order constraints over  $\mathcal{L}$ . A solution  $\mathcal{A}$  satisfies  $(\mathcal{L}, \mathcal{M}, \mathcal{X}, \mathcal{C})$  iff  $\mathcal{M} \models c_j[\mathcal{A}]$  for all  $c_j \in \mathcal{C}$ .*

**Grounding and Reduction.** To connect with the propositional SAT/CSP framework, FOL-CSPs are grounded by instantiating quantifiers over finite domains, yielding large but finite propositional subproblems. Formally, each quantified constraint

$$Q_1 y_1 \dots Q_r y_r \psi_j(x_1, \dots, x_k, y_1, \dots, y_r)$$

is converted into a finite set of propositional clauses

$$\{\psi_j(x_1, \dots, x_k, a_1, \dots, a_r) \mid a_i \in \mathcal{U}\},$$

where  $\mathcal{U}$  is the domain of instantiation. Learned clause priors and predicate embeddings guide this process by ranking likely instantiations, thus reducing combinatorial explosion and improving solver efficiency. This concept is applied in Algorithm 18 (S1<sub>18</sub>) for clause prioritization and grounding selection, and in Algorithm 11 (S0<sub>11</sub>) for CNF feature extraction before propagation.

**Neural Assistance.** This paragraph introduces neural predicate encoders such as GNNs and Transformers, which produce clause embeddings  $\phi(\mathcal{K}, q)$  and predict satisfiability probabilities  $p_\theta(q|\mathcal{K})$ . This mechanism is implemented in Algorithm 18 (S0<sub>18</sub>, S1<sub>18</sub>) to rank quantified clauses.

Recent neuro-symbolic solvers [40] represent predicates, constants, and relations as nodes in a relational graph and employ GNNs or Transformer encoders to predict the relevance or satisfiability probability of each clause. Given a knowledge base  $\mathcal{K}$  and a query  $q$ , a neural model estimates the entailment likelihood

$$p_\theta(q \mid \mathcal{K}) = \sigma(\mathbf{w}^\top \phi(\mathcal{K}, q)),$$

where  $\phi(\mathcal{K}, q)$  is an embedding of the symbolic-graph pair,  $\mathbf{w}$  and  $\theta$  are trainable parameters, and  $\sigma(\cdot)$  is the logistic activation. The resulting probabilities serve as priorities for clause selection and grounding order.

**Integration with the Unified ML–CSP Framework.** This paragraph links neural models with classical LCG/CDCL solvers, describing a feedback loop where

learned clause relevance guides grounding and solver conflicts update neural encoders. This integration is realized in Algorithm 18 (S<sub>0</sub><sub>18</sub>–S<sub>3</sub><sub>18</sub>) and further operationalized in Algorithm 13 (S<sub>3</sub><sub>13</sub>) for feedback-driven clause evaluation.

Within the overall framework, FOL-CSPs extend the ML-enhanced LCG/CDCL loop: (1) neural relevance models rank quantified clauses before grounding, (2) grounding produces propositional constraints used by the standard solver, and (3) feedback from solver conflicts updates the neural encoders. This establishes a recursive interaction between symbolic deduction and statistical learning.

The operation of this neuro-symbolic FOL-CSP module is summarized in Algorithm 18. Each step mirrors the solver phase style (S<sub>0</sub><sub>18</sub>–S<sub>3</sub><sub>18</sub>) used throughout the paper.

---

#### Algorithm 18 Neural-Assisted FOL-CSP Inference

---

##### Initialization

(S<sub>0</sub><sub>18</sub>) Construct the relational graph  $\mathcal{G} = (V_{\text{var}} \cup V_{\text{pred}}, E)$  from  $\mathcal{M}$  or knowledge base  $\mathcal{K}$ . Initialize a neural encoder  $\phi_\theta$  that produces predicate and clause embeddings, and a relevance predictor  $p_\theta(c_j)$  estimating the usefulness of each constraint.

##### Clause Prioritization

(S<sub>1</sub><sub>18</sub>) Rank constraints by their predicted relevance  $p_\theta(c_j)$ . Select the top- $K$  clauses or those with  $p_\theta(c_j) > \tau$  for grounding. Generate partial propositional encodings for these high-confidence clauses.

##### Guided Symbolic Search

(S<sub>2</sub><sub>18</sub>) Perform unification and substitution among selected clauses. Neural similarity between predicate embeddings guides the order of resolution. Conflicts or failed unifications are recorded to refine  $\phi_\theta$ .

##### Integration with Propositional Solvers

(S<sub>3</sub><sub>18</sub>) The grounded propositional subset  $\mathcal{C}_{\text{grounded}}$  is forwarded to the ML-enhanced LCG/CDCL solver. Backpropagated signals from solver conflicts update neural parameters  $\theta$ , closing the loop between symbolic and statistical reasoning.

##### Termination

The procedure terminates when all clauses are either satisfied or grounded. If all constraints are satisfied under some assignment  $\mathcal{A}$ , return SAT; otherwise return UNSAT.

---

This paragraph summarizes the hierarchical solver structure corresponding to Algorithm 18 (S<sub>0</sub><sub>18</sub>–S<sub>3</sub><sub>18</sub>): (S<sub>0</sub><sub>18</sub>) relational graph construction, (S<sub>1</sub><sub>18</sub>) clause relevance estimation, (S<sub>2</sub><sub>18</sub>) symbolic–neural unification, and (S<sub>3</sub><sub>18</sub>) integration with propositional solvers.

**Connection to the Global Framework.** This paragraph explains the integrative role of the FOL-CSP module in the overall architecture, corresponding conceptually to Algorithm 11 ( $S_{011}$ ). It describes how the FOL-CSP layer bridges propositional reasoning at the SAT level and dynamic optimization at the planning level through ML-RL interaction, establishing a unified constraint-solving pipeline. Formally, the integration preserves a hierarchical dependency:

$$\text{Symbolic Reasoning} \rightarrow \text{FOL-CSP} \rightarrow \text{RL/DynP}.$$

By embedding symbolic inference within this ML-RL hierarchy, the framework provides a continuous flow of information from logical clauses to sequential decision policies, supporting consistent reasoning, planning, and scheduling under uncertainty.

## 9 Empirical Evidence from the Literature

To strengthen the theoretical framework introduced in this paper, this section summarizes and analyzes empirical findings reported in prior studies on machine learning-assisted constraint solving and combinatorial optimization. These works collectively demonstrate that data-driven and hybrid symbolic-learning approaches can substantially enhance solver efficiency, scalability, and adaptability.

### 9.1 RL for Search Heuristics

RL has been repeatedly shown to improve the efficiency of combinatorial and scheduling solvers. For example, Park et al. [38] and Liu et al. [33] combined GNNs with deep RL policies to learn dispatching rules for the job-shop scheduling problem, achieving faster convergence and reduced makespan compared to traditional heuristics. Chen et al. [14] proposed an attention-based RL framework with disjunctive graph embeddings that reduced tardiness and outperformed metaheuristic baselines. In chemical production scheduling, Mowbray et al. [36] used distributional RL to optimize batch sequencing under uncertainty, showing robust performance against domain-specific solvers. These results confirm that RL-guided heuristic selection can effectively replace handcrafted rules in dynamic and stochastic scheduling domains.

### 9.2 ML for SAT and CSP Solvers

A substantial body of empirical work demonstrates that machine learning can significantly improve SAT and CSP solver performance. Liang’s PhD thesis [31]

and follow-up works such as Audemard and Simon [3], Liang et al. [32], and Bergin et al. [8] showed that learned branching heuristics and clause-quality predictors yield faster convergence on benchmark families. Selsam et al. [46] introduced the **NeuroSAT** architecture, which learns unsupervised message-passing embeddings to predict satisfiability, achieving competitive accuracy across standard **SATLIB**<sup>1</sup> and handcrafted datasets. Subsequent transformer-based extensions [47, 48] further improved scalability and runtime performance on industrial SAT instances. Matos et al. [34] successfully applied a hybrid SAT and ML pipeline to periodic timetabling, reducing solution time and improving feasibility rates on public transport data. Together, these studies empirically validate that data-driven branching, clause learning, and variable selection can improve search efficiency in Boolean and finite-domain constraint satisfaction problems.

### 9.3 Neural and Hybrid Optimization Frameworks

Several works demonstrate the integration of neural architectures with symbolic optimization models. Oh et al. [23] employed a ML-based disjunctive model for static program analysis, achieving higher accuracy and reduced false positives relative to purely symbolic approaches. Recent advances in physics-inspired and graph-based neural solvers further validate this paradigm: Krutský et al. [29] binarized physics-inspired GNNs for large-scale combinatorial optimization, achieving competitive accuracy with substantially reduced model size. The empirical evaluations in these studies demonstrate that learned neural representations can effectively approximate or complement the symbolic reasoning process underlying classical solvers.

### 9.4 Summary of Reported Improvements

Table 3 consolidates representative empirical results from the literature that support the feasibility of ML- and RL-assisted constraint solving. The reported improvements consistently indicate significant reductions in search effort and runtime compared with traditional handcrafted heuristics.

---

<sup>1</sup><http://www.cs.ubc.ca/~hoos/SATLIB/>

Table 3: Representative empirical results supporting ML-assisted constraint solving.

Reference	Summary of Empirical Findings
Park et al. (2021) [38]	<b>Approach:</b> GNN + RL scheduling policy <b>Problem Domain:</b> Job-shop scheduling <b>Reported Improvement:</b> 10–25% makespan reduction
Liu et al. (2023) [33]	<b>Approach:</b> Deep RL with GNN features <b>Problem Domain:</b> Dynamic JSSP <b>Reported Improvement:</b> 20–35% runtime improvement
Chen et al. (2023) [14]	<b>Approach:</b> Attention-based RL + disjunctive graph <b>Problem Domain:</b> Job-shop scheduling <b>Reported Improvement:</b> Reduced tardiness by 30%
Liang et al. (2016) [32]	<b>Approach:</b> ML-guided branching heuristic <b>Problem Domain:</b> SAT solving <b>Reported Improvement:</b> Faster solving on industrial benchmarks
Selsam et al. (2018) [46]	<b>Approach:</b> Message-passing GNN (NeuroSAT) <b>Problem Domain:</b> SAT, CSP classification <b>Reported Improvement:</b> Accurate satisfiability prediction
Matos et al. (2021) [34]	<b>Approach:</b> ML + SAT hybrid optimization <b>Problem Domain:</b> Timetabling <b>Reported Improvement:</b> Shorter runtime, higher feasibility
Oh et al. (2019) [23]	<b>Approach:</b> ML-enhanced disjunctive model <b>Problem Domain:</b> Program analysis <b>Reported Improvement:</b> Improved precision, fewer false alarms
Continued on next page	

**Table 3 (continued)**

Reference	Summary of Empirical Findings
Krutský et al. (2025) [29]	<p><b>Approach:</b> Binarized physics-inspired GNN</p> <p><b>Problem Domain:</b> Combinatorial optimization</p> <p><b>Reported Improvement:</b> Comparable accuracy, lower compute cost</p>

**Acknowledgements** This work received funding from the National Centre for Energy II (TN02000025).

## References

- [1] Muhammad Abdullah Adnan, Ryo Sugihara, and Rajesh K. Gupta. Energy efficient geographical load balancing via dynamic deferral of workload. In *2012 IEEE Fifth International Conference on Cloud Computing*, pages 188–195, 2012.
- [2] Krzysztof R Apt and Mark Wallace. *Constraint logic programming using ECLiPSe*. Cambridge University Press, 2006.
- [3] Gilles Audemard and Laurent Simon. Predicting learnt clauses quality in modern sat solvers. In *International Joint Conference on Artificial Intelligence (IJCAI)*, pages 399–404, 2009.
- [4] Egon Balas. *Disjunctive Programming*. Springer International Publishing, 2018.
- [5] Jørgen Bang-Jensen and Gregory Z Gutin. *Digraphs: theory, algorithms and applications*. Springer Science & Business Media, 2008.
- [6] Dina Barak-Pelleg and Daniel Berend. On the satisfiability threshold of random community-structured sat. pages 1249–1255, 2018.
- [7] Anton Beloglazov, Jemal Abawajy, and Rajkumar Buyya. Energy-aware resource allocation heuristics for efficient management of data centers for cloud computing. *Future Generation Computer Systems*, 28(5):755–768, May 2012.
- [8] Ruth Helen Bergin, Marco Dalla, Andrea Visentin, Barry O’Sullivan, and Gregory Provan. Using machine learning classifiers in sat branching. In *Proceedings of the International Symposium on Combinatorial Search*, volume 16, pages 169–170, 2023.

- [9] Filip Beskyd and Pavel Surynek. Parameter setting in sat solver using machine learning techniques. In *Proceedings of the 14th International Conference on Agents and Artificial Intelligence*, page 586–597. SCITEPRESS - Science and Technology Publications, 2022.
- [10] Armin Biere. Picosat essentials. *Journal on Satisfiability, Boolean Modeling and Computation (JSAT)*, 4:75–97, 2008.
- [11] Armin Biere, Katalin Fazekas, Mathias Fleury, and Maximilian Heisinger. CaDiCaL, Kissat, Paracooba, Plingeling and Treengeling entering the SAT competition 2020. In Tomáš Balyo, Matti Järvisalo, and Markus Iser, editors, *Proceedings of SAT Competition 2020 – Solver and Benchmark Descriptions*, volume B-2020-1 of *Department of Computer Science Report Series B*, pages 4–12, Helsinki, Finland, 2020. University of Helsinki.
- [12] John Adrian Bondy and Uppaluri Siva Ramachandra Murty. *Graph theory*. Springer Publishing Company, Incorporated, 2008.
- [13] Andreas Bueff and Vaishak Belle. Deep inductive logic programming meets reinforcement learning. In *Proceedings of the 39th International Conference on Logic Programming (ICLP 2023)*, volume 385 of *EPTCS*, pages 339–352, 2023.
- [14] Ruiqi Chen, Wenxin Li, and Hongbing Yang. A deep reinforcement learning framework based on an attention mechanism and disjunctive graph embedding for the job-shop scheduling problem. *IEEE Transactions on Industrial Informatics*, 19(2):1322–1334, 2023.
- [15] Márk Danisovszky, Zijian Gyozo Yang, and Gábor Kusper. Classification of sat problem instances by machine learning methods. In *ICAI*, pages 94–104, 2020.
- [16] Leonardo De Moura and Nikolaj Bjørner. Z3: An efficient smt solver. In *International conference on Tools and Algorithms for the Construction and Analysis of Systems*, pages 337–340. Springer, 2008.
- [17] Bruno Dutertre and Leonardo de Moura. The yices smt solver. In *Proceedings of the Satisfiability Modulo Theories Workshop (SMT)*, 2006.
- [18] Niklas Eén and Niklas Sörensson. An extensible sat-solver. In *Theory and Applications of Satisfiability Testing (SAT)*, volume 2919 of *Lecture Notes in Computer Science*, pages 502–518. Springer, 2004.
- [19] Justin Gilmer, Samuel S Schoenholz, Patrick F Riley, Oriol Vinyals, and George E Dahl. Neural message passing for quantum chemistry. In *International conference on machine learning*, pages 1263–1272. Pmlr, 2017.
- [20] Alexander Grigor’yan, Yong Lin, Yuri Muranov, and Shing-Tung Yau. Cohomology of digraphs and (undirected) graphs. *Asian Journal of Mathematics*, 19(5):887–932, 2015.

- [21] Aditya Grover and Jure Leskovec. node2vec: Scalable feature learning for networks. In *Proceedings of the 22nd ACM SIGKDD International Conference on Knowledge Discovery and Data Mining*, KDD '16, page 855–864. ACM, August 2016.
- [22] Milan Janić. *Advanced transport systems*. Springer, 2014.
- [23] Minseok Jeon, Sehun Jeong, Sungdeok Cha, and Hakjoo Oh. A machine-learning algorithm with disjunctive model for data-driven program analysis. *ACM Transactions on Programming Languages and Systems*, 41(2):13:1–13:41, 2019.
- [24] Morteza Kimiaeи and Vyacheslav Kungurtsev. Machine Learning Algorithms for Assisting Solvers for Constraint Satisfaction Problems. Optimization Online E-Print Repository, November 2025. ID: 32520.
- [25] Morteza Kimiaeи and Vyacheslav Kungurtsev. Supplementary material for *Machine Learning Algorithms for Assisting Solvers for Constraint Satisfaction Problems*. [https://github.com/GS1400/suppMat\\_ML\\_CSP](https://github.com/GS1400/suppMat_ML_CSP), 2025. Supplementary material; accessed: 2025-11-30.
- [26] Diederik P. Kingma and Jimmy Ba. Adam: A method for stochastic optimization. *International Conference on Learning Representations (ICLR)*, 2015.
- [27] TN Kipf. Semi-supervised classification with graph convolutional networks. *arXiv preprint arXiv:1609.02907*, 2016.
- [28] Bernhard Korte and Jens Vygen. *Combinatorial Optimization: Theory and Algorithms*. Springer, 4th edition, 2007. A classic book providing a theoretical foundation for combinatorial optimization problems.
- [29] Martin Krutský, Gustav Šír, Vyacheslav Kungurtsev, and Georgios Korpas. Binarizing physics-inspired gnns for combinatorial optimization. *arXiv preprint arXiv:2507.13703*, 2025.
- [30] Jingyan Li, Yuri Muranov, Jie Wu, and Shing-Tung Yau. On singular homology theories of digraphs and quivers. Technical report, Yanqi Lake Beijing Institute of Mathematical Sciences and Applications (BIMSA), Beijing, China, 2024. Preprint, BIMSA Publication No. 5381.
- [31] Jia Hui Liang. *Machine Learning for SAT Solvers*. Phd thesis, University of Waterloo, 2018.
- [32] Jia Hui Liang, Vijay Ganesh, Pascal Poupart, and Krzysztof Czarnecki. Learning rate based branching heuristic for sat solvers. In *International Conference on Theory and Applications of Satisfiability Testing*, pages 123–140. Springer, 2016.

- [33] Chien-Liang Liu and Tzu-Hsuan Huang. Dynamic job-shop scheduling problems using graph neural network and deep reinforcement learning. *IEEE Transactions on Systems, Man, and Cybernetics: Systems*, 53(11):6836–6849, 2023.
- [34] Gonçalo P. Matos, Luís M. Albino, Ricardo L. Saldanha, and Ernesto M. Morgado. Solving periodic timetabling problems with sat and machine learning. *Public Transport*, 13(3):625–648, 2021.
- [35] Volodymyr Mnih, Adrià Puigdomènech Badia, Mehdi Mirza, Alex Graves, Timothy Lillicrap, Tim Harley, David Silver, and Koray Kavukcuoglu. Asynchronous methods for deep reinforcement learning. In *Proceedings of the 33rd International Conference on Machine Learning (ICML)*, volume 48 of *Proceedings of Machine Learning Research*, pages 1928–1937. PMLR, 2016. No DOI assigned; official PMLR version.
- [36] Max Mowbray, Dongda Zhang, and Ehecatl Antonio Del Rio Chanona. Distributional reinforcement learning for scheduling of chemical production processes. 2022.
- [37] Nina Narodytska, Alexey Ignatiev, Filipe Pereira, and Joao Marques-Silva. Learning optimal decision trees with sat. In *Proceedings of the 27th International Joint Conference on Artificial Intelligence (IJCAI-18)*, pages 1362–1368. IJCAI Organization, 2018.
- [38] Junyoung Park, Jaehyeong Chun, Sang Hun Kim, Youngkook Kim, and Jinkyoo Park. Learning to schedule job-shop problems: representation and policy learning using graph neural network and reinforcement learning. *International Journal of Production Research*, 59(11):3360–3377, 2021.
- [39] Michael Patriksson. *The Traffic Assignment Problem: Models and Methods*. Dover Publications, revised edition edition, 2015. Covers models and optimization methods for traffic assignment and routing problems.
- [40] Tim Rocktäschel and Sebastian Riedel. End-to-end differentiable proving. *Advances in Neural Information Processing Systems*, 30, 2017. NeurIPS 2017.
- [41] Stuart J. Russell and Peter Norvig. *Artificial Intelligence: A Modern Approach*. Pearson Education Limited, Harlow, England, 4th, global edition edition, 2021.
- [42] Karen Scarfone and Peter Mell. *Guide to Intrusion Detection and Prevention Systems (IDPS)*. National Institute of Standards and Technology (NIST), 2007. A comprehensive guide to intrusion detection and prevention systems, including network security models and techniques.
- [43] John Schulman, Filip Wolski, Prafulla Dhariwal, Alec Radford, and Oleg Klimov. Proximal policy optimization algorithms. In *Proceedings of the 34th International Conference on Machine Learning (ICML)*, 2017.

- [44] Christian Schulte, Mikael Lagerkvist, and Guido Tack. Gecode: Generic constraint development environment. <https://www.gecode.org>, 2006. Accessed: 2025-11-04.
- [45] Daniel Selsam and Nikolaj Bjørner. *Guiding High-Performance SAT Solvers with Unsat-Core Predictions*, page 336–353. Springer International Publishing, 2019.
- [46] Daniel Selsam, Matthew Lamm, Benedikt Bünz, Percy Liang, Leonardo de Moura, and David L Dill. Learning a sat solver from single-bit supervision. *arXiv preprint arXiv:1802.03685*, 2018.
- [47] Feng Shi, Chonghan Lee, Mohammad Khairul Bashar, Nikhil Shukla, Song-Chun Zhu, and Vijaykrishnan Narayanan. Transformer-based machine learning for fast sat solvers and logic synthesis. *arXiv preprint arXiv:2107.07116*, 2021.
- [48] Zhengyuan Shi, Min Li, Sadaf Khan, Hui-Ling Zhen, Mingxuan Yuan, and Qiang Xu. Satformer: Transformers for sat solving. *arXiv preprint arXiv:2209.00953*, 2022.
- [49] Mate Soos, Karsten Nohl, and Claude Castelluccia. Extending sat solvers to cryptographic problems. In *International Conference on Theory and Applications of Satisfiability Testing*, pages 244–257. Springer, 2009.
- [50] Peter J. Stuckey, Andreas Schutt, Thorsten Ehlers, Graeme Gange, Kathryn Francis, and Geoffrey Chu. Chuffed: A lazy clause generation solver. <https://github.com/chuffed/chuffed>, 2018. Accessed: 2025-11-04.
- [51] Ling Sun, David Gerault, Adrien Benamira, and Thomas Peyrin. Neurogft: Using a machine learning based sat solver for cryptanalysis. In *Proceedings of the 4th International Symposium on Cyber Security Cryptography and Machine Learning (CSCML 2020)*, volume 12161 of *Lecture Notes in Computer Science*, pages 62–78. Springer, 2020.
- [52] Richard S. Sutton and Andrew G. Barto. *Reinforcement Learning: An Introduction*. MIT Press, Cambridge, MA, 2nd edition, 2018.
- [53] Aviv Tamar, Yonatan Glassner, and Shie Mannor. Optimizing the cvar via sampling. In *Proceedings of the AAAI Conference on Artificial Intelligence*, volume 29, 2015.
- [54] Petar Veličković, Guillem Cucurull, Arantxa Casanova, Adriana Romero, Pietro Lio, and Yoshua Bengio. Graph attention networks. *arXiv preprint arXiv:1710.10903*, 2017.
- [55] Oriol Vinyals, Meire Fortunato, and Navdeep Jaitly. Pointer networks. In *Advances in Neural Information Processing Systems (NeurIPS)*, volume 28, pages 2692–2700. Curran Associates, Inc., 2015.

- [56] Haoze Wu. Improving sat-solving with machine learning. In *Proceedings of the 2017 ACM SIGCSE Technical Symposium on Computer Science Education*, SIGCSE '17, page 787–788. ACM, March 2017.
- [57] Keyulu Xu, Weihua Hu, Jure Leskovec, and Stefanie Jegelka. How powerful are graph neural networks? *arXiv preprint arXiv:1810.00826*, 2018.
- [58] Qing Zhao and Behnaam Aazhang. *Dynamic Spectrum Access in Wireless Networks: A Survey*, volume 7 of *Wireless Communications and Mobile Computing*. Springer, 2007. Explores dynamic spectrum allocation in wireless networks, providing models and optimization methods.
- [59] Neng-Fa Zhou, Cristian Grozea, Håkan Kjellerstrand, and Oisín Mac Fhearaí. Picat through the lens of advent of code. *arXiv preprint arXiv:2507.11731*, 2025.